Politecnico di Torino

Master of Science in Energy and Nuclear Engineering

Master Thesis

Comparison of dosimetric approaches in liver radioembolization

Supervisors:

Prof. Gianni Coppa

Prof.ssa Desirée Deandreis (Università degli studi di Torino)

Dott.ssa Monica Finessi

(A.O.U. Città della Salute e della Scienza di Torino)

Candidate:

Mariacarla D'Orazio

Academic year 2020/2021

Acknowledgements

I would like to thank Dott.ssa Monica Finessi and Dott.ssa Desirée Deandreis (Molinette Hospital) for support and availability. Despite difficulties due to pandemic period, it was possible to collaborate remotely.

Also like to thank Prof. Gianni Coppa (Politecnico di Torino) for the help and the academic support in the thesis work.

Finally, thanks to all the people who were close to me in the period of thesis.

Contents

Abstract

The scientific research work of this thesis was developed at University Nuclear Medicine Division of the Department of Medical Sciences at Molinette hospital of Turin. Three dosimetric methods were performed (MIRD, VOXEL, Simplicity) for the hepatic radioembolization with yttrium-90. The study cases were 13 patients (12 males and 1 female) suffering from hepatocellular carcinoma with an average age of 64 years (51-83). Data was collected between June 2019 and April 2021.

For ^{90}Y-TARE glass spheres were injected through a catheter via hepatic artery. The treatment was compound from pre-treatment, treatment, post-treatment, and follow-up. All the steps are performed in the University Nuclear Medicine Division of the Department of Medical Sciences at Molinette hospital of Turin.

The study is divided in retrospective and prospective phases. The first is used in the pre-treatment for the evaluation of the radiopharmaceutical activity, which should be administered to the target, and the eligibility of the patient. The second is performed after the administration to verify the isotope distribution and the absorbed dose in the liver.

The obtained results show that for the dosimetric evaluation the three methods (MIRD, VOXEL, Simplicity) have not differences. Dosimetric limits are respected, both for patient-related safety and for efficacy. The choice of the methods depends on the availability of software in the hospital.

Sommario

Il lavoro di ricerca scientifica di questa tesi è stato sviluppato presso il Dipartimento di Medicina Nucleare del Dipartimento di Scienze Mediche dell'Ospedale Molinette di Torino. Sono stati analizzati tre metodi dosimetrici (MIRD, VOXEL e Simplicity) nella radioembolizzazione epatica con ittrio-90. I casi studio sono stati 13 pazienti (12 maschi e 1 femmina) affetti da carcinoma epatocellulare con età media di 64 anni (51-83). I dati sono stati raccolti nel periodo tra giugno 2019 ed aprile 2021.

Per la terapia di radioembolizzazione sono state utilizzate sfere di vetro di ittrio-90, inserite nel paziente attraverso un catetere tramite l'arteria epatica. La terapia è composta da una fase di pretrattamento, una relativa al trattamento, una post trattamento ed una finale di follow-up del paziente. Tutti gli step vengono effettuati nel Dipartimento di Medicina Nucleare del Dipartimento di Scienze Mediche dell'Ospedale Molinette di Torino.

Lo studio si divide in una fase retrospettiva ed una prospettica. La prima viene svolta nella fase preliminare del trattamento per valutare l'attività del radiofarmaco necessaria da somministrare al target e l'idoneità del paziente al protocollo. La seconda viene svolta dopo la somministrazione per verificare la distribuzione dell'isotopo e la dose rilasciata nel fegato.

I risultati ottenuti dall'analisi condotta con i tre metodi evidenziano che la valutazione dosimetrica non ha sostanziali differenze per i metodi MIRD, VOXEL e Simplicity e che i limiti dosimetrici sono rispettati, sia per la sicurezza legata al paziente e sia per l'efficacia. La scelta relativa a quale metodo adottare spetta all'operatore sanitario di Medicina Nucleare, in base alla disponibilità dei software nell'ospedale.

Introduction

The International Commission on Radiological Protection (ICRP) and the International Commission on Radiation Units and Measurements (ICRU) have elaborated dosimetric quantities to estimate radiation doses from internal and external radiation exposures [1]. For ICRP the central dosimetric quantities are related to the measure of energy imparted to organs and tissues in the body, which were adopted in 1977 Recommendations and then in 1990 Recommendations [1].

In nuclear medicine, radiations are employed for diagnostic and for treatment purposes, especially in the oncological field. In therapeutic nuclear medicine it is relevant and mandatory for European law (2013/59 EURATOM) [2] to perform dosimetric evaluations. With the goal to reduce the absorbed dose from healthy tissue and to optimize efficacy of the medical applications. In fact, on one side the exposure to ionizing radiations can induce short term and old long-term effects on health [1]. If the dose delivered especially regarding healthy organ is too high, a damage to organs, cells and tissues can occur with a higher cumulative risk to develop toxicities, that in some cases can be fatal such as the development of second induced cancer. On the other side if the delivered dose to the target is not sufficiently high, the therapeutic effect can be limited.

This work is focused on the different dosimetric methods to estimate the dose delivered to hepatocellular carcinoma (HCC) and to healthy tissues from Transarterial Radioembolisation (TARE) by ^{90}Y microspheres.

The hepatocellular carcinoma is the fifth most common cancer in the world [3]. There are different treatments to cure hepatic cancer, according to different tumour stage, both through systemic or loco-regional treatment. ^{90}Y -TARE is a very effective option for loco-regional treatment of HCC.

The study was performed at University Nuclear Medicine Division of the Department of Medical Sciences at Molinette hospital. The Molinette hospital is part of largest pole at national and European level, “A.O.U. Città della Salute e della Scienza di Torino”. In the Nuclear Medicine Division both diagnostic examination and therapies are performed through the administration of different radiopharmaceuticals in patients. A data collection of patients treated with ^{90}Y TARE from June 2019 to April 2021 has been conducted. In particular the aim of the study was to compare dosimetric data obtained for the evaluation

of the absorbed doses in the patient through different dosimetric methods (MIRD, VOXEL) applying different software available: MATLAB and Simplicity®. With the aim to respect the limit of 80-120 Gy to healthy liver and 30 Gy to lungs [3], and to find if there are differences between them.

Chapter 1

1 Medical application of radiation

Nuclear medicine therapy is used to treat cancer that usually is combined with other treatment options, such as chemotherapy and surgery. Among the most important characteristics to be considered in the choice of radionuclide for therapy are the type of particle emitted (mainly β- or alpha), the physical half-time and the energy. These last characteristics are important because a too low energy associated with a too short half-life can prevent the release of an insufficient dose to the target obtain any therapeutic effect, on the other hand, a too high energy can lead the emitted particle to travel a path too long in the tissues before being absorbed, causing damage to the tissues surrounding the therapeutic "target".

Using high doses, it is possible to kill cancer cells or reduce the tumour mass and it is used to stop its growth. The dead of the tumour cells is driven by the damage of their DNA. This procedure is not instantaneous, but it takes some days or weeks before the total destroying of cancer cells.

The administration of radiation needs some precise limits to ensure a safe treatment. The dose must be balanced between absorbed dose from target volumes and the received dose from healthy tissue. There are side effects of radiation in human body because there are killed not only the cancer cells, but radiation can also kill the healthy cells. For this reason, it is necessary to keep radiation doses as low as reasonably achievable (ALARA), minimizing the exposure time.

The absorbed dose equilibrium is necessary to avoid some risks: the disease underdosing, which means an ineffective therapy, or the overdosing that can cause long term toxicity [4].

There are two types of radiation therapy available: external beam radiation therapy (EBRT) and internal radiation therapy (IRT). The choice of the therapy depends on the clinical needs, on the type of tumour, on the dimensions and on the location in the patient body [5].

1.1 External beam radiation therapy

This kind of therapy is used to treat different cancer types. The radiation is delivered to a localized area, where there is the cancer, and it means that this external approach is local [5]. The beams are generated by a linear accelerator and deliver high-energy x-ray or electron beam to the target. With the microwaves technology the accelerator speeds up the electrons, which interact with a heavy metal target to generate high-energy x-rays.

Furthermore, the accelerator exit has the shape of the area of the body that should be treated by the therapy.

In this treatment there are employed different beams that come from photons, protons, or electrons. The photons and the protons beams can reach tumours that are in deep area in the body. The electron beam might not travel faraway in tissues. Due to its small penetration, this kind of radiation is used for a skin tumour or for cancer in the surface of the body [5].

External beam therapy is applied in fractionated administrations. This allows healthy cells to recover and to obtain a more effective radiation of the target. The administration to the patient it is made in the hospital, and it is not necessary to stay the night. Furthermore, this therapy does not make the patient radioactive.

1.2 Internal radiation therapy

There are two different types of internal radiation therapy: brachytherapy and radioembolization.

Brachytherapy

In brachytherapy a sealed solid source is applied and this kind of therapy it is conducted by the insertion of the source in a specific place of the body by the means of capsules [5].

The injection of the pharmaceutical it is triggered by different procedures: interstitial, intracavity or episcleral brachytherapy. The first introduces the source in the tumour area, for prostate cancer. Instead, the intracavity technique inserts the radiation source in a body cavity or in a cavity created and it is used for cervical cancer. The last method places the source in the eye to cure ocular melanoma [5].

The positioning of the radiation source is performed with a catheter. When the radiopharmaceutical is placed, it can be stay in the patient for minutes, days or for the rest of the life. The difference is made by the dose rate of the implants: low-dose, high-dose or permanent.

If the patient receives a high dose, he may need to stay isolated from other people because his body emits radiation after the treatment [5].

Radioembolization

This therapy is safe and efficacious treatment modality for unresectable primary and secondary liver tumours using Yttrium-90 (^{90}Y)-microspheres of resin or glass. The microspheres are delivered to the tumour through trans-arterial administration in order to irradiate locally the lesion, preserving normal tissue. ^{90}Y is a pure beta-emitting radionuclide with a physical half-life ($T_{1/2}$) of 64.2 hours. About 94% of the ^{90}Y radiation dose is delivered during the first 11 days following treatment.

1.3 Systemic Radionuclide therapy

The systemic radionuclide therapy uses radioactive drugs to treat different type of more advanced cancers. Whit a liquid radioactive pharmaceutical, the administration to the patient is made by mouth or through the vein [6]. This therapy employs unsealed radioactive substance, which crossed the whole body and delivers radiation to several targets. Systemic therapy means that the radiation is diffused in several zones, and it is not a targeted treatment.

The therapy is made by radioactive iodine or ^{177}Lu peptide receptor radionuclide therapy. Peptide receptor radionuclide therapy (PRRT) is another pharmaceutical which binds the radioactive material with peptide, which is a protein [6].

1.4 Dosimetric parameters

Analysing ionizing radiation and their applications, it is relevant to introduce parameters which give knowledges about the dose released in the body. The aim of dosimetric analysis is to reduce the amount of energy released in the tissues and to limit the normal tissue damage.

1.4.1 Absorbed dose

The absorbed dose is defined as the energy imparted by ionising radiation for unit mass from internal emitters, it is called with D, which is defined in the equation 1 [1]. The deposited dose in tissues depends on the type of particles emitted by isotope decay and on the activity. The SI unit measure is the Gray (Gy), it is Joule per kilogram [1]. In older notation, the absorbed dose is expressed with rad (100 rad=1 Gy).

$$D = \frac{dE}{dm} \tag{1}$$

1.4.2 Equivalent dose and effective dose

The equivalent dose considers the type of radiation, it comes from the product between the absorbed dose and the radiation type factor. Moreover, it is possible to compute this dose with the equation 2 [1].

$$H_T = \sum_R w_R D_{T,R} \tag{2}$$

Where $D_{T,R}$ is the absorbed dose and w_R is the radiation weighting factor, which depends on the radiation type R. The SI unit measure is the Sievert (Sv), in older notation it is used rem (100 rem= 1 Sv), it is Joule per kilogram [1]. The proposed radiation weighting factors in Recommendations are in table 1 [1].

Radiation type	Radiation weighting factor, w_R
Photons	1
Electrons and muons	1
Protons	2
Alpha particles, fission fragments, heavy nuclei	20
Neutrons	A continuous curve depending on neutron energy is recommended (see Figure 2 and equation 4.7)

Table 1

The equivalent dose multiplied by the tissue weighting factor represents the effective dose. This can be measured by the equation 3 [1].

$$E = \sum_{T} w_T \sum_{R} w_R D_{T,R} \tag{3}$$

Where w_T represents the tissue weighting factor. It is taken the sum of all contributes to consider the radiation impact on the different organs in the body. The unit measure of the effective dose is the same of the equivalent dose. In table 2 [1] there are listed the tissue weighting factors from ICRP Recommendations.

Tissue	w_T	$\sum w_T$
Red bone marrow, colon, lung, stomach, Remainder Tissues* (Nominal w_T applied to the average dose to 15 tissues)	0.12	0.60
Breast, Gonads	0.08	0.16
Bladder, oesophagus, liver, thyroid	0.05	0.20
Bone surface, brain, salivary glands, skin	0.01	0.04

Table 2

1.4.3 Biological effects of radiation

Radiation can be direct, which causes the DNA damage and the cells death, or it can be indirect, that destroys DNA with the formation of free radicals.

The fraction of dead cells it depends on the type of radiation, on its energy, on the released dose and on the kind of irradiated cells.

DNA is made by two strands and radiation can broke one of them or both. If a particle passes through one strand and it damages the string, after a certain time it is repaired, so DNA is not harmed. Moreover, if one particle, or two different particles crosse both the strands, there is a permanent damage and DNA cannot be repaired anymore.

The linear-quadratic model is used to find the cell survival probability which is exposed to a single dose of radiation [7]. The equation 4 takes in relationship the cell survival and the released dose:

$$S = e^{-\alpha D - \beta D^2} \tag{4}$$

where α and β represent the cell's radiosensitivity, however D is the exposure dose.

Plotting survival behaviour on a log scale, this leads a quadratic curve, as in the figure 1 [7].

The α reflects the cell death for one single hit event, while β is refers to multiple hit events. The ratio of these two quantities is expressed in Gy, and it is the dose at which α and β are the same.

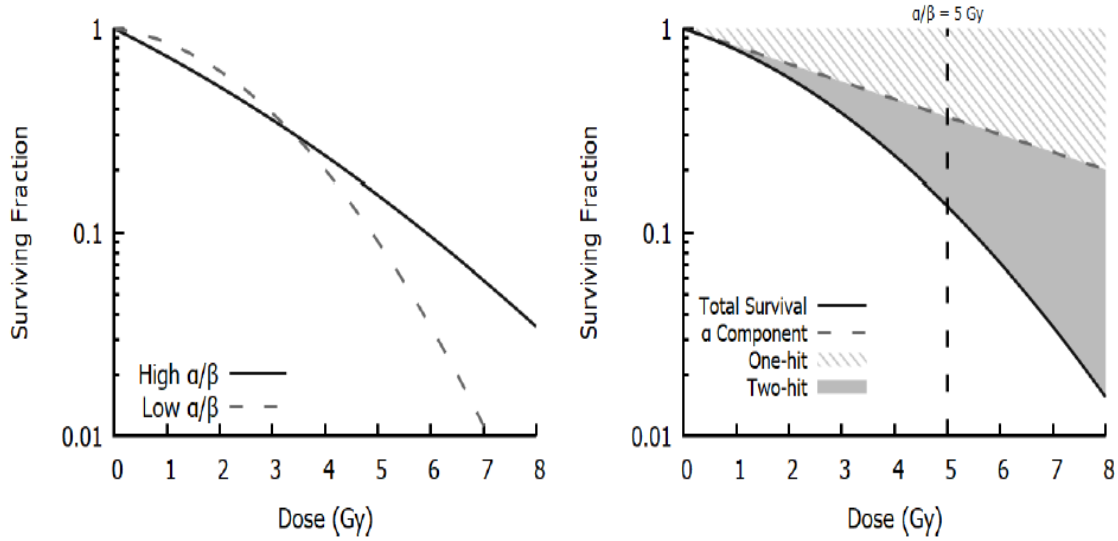

Figure 1 The left illustration lays out cell lines with α/β high and low ratios. The continuous line it is for high ratio (10 Gy), it has nearly constant rates of cells that are killed with increasing dose, while dotted line (3 Gy) shows a greater killing dose at higher dose per unit dose. In right graph there are reported two different areas for one or two hit events. One hit is more important for low doses, in contrast two hit events are relevant for higher dose [7].

In the previous formula, S is the probability that a cell receives n hits after an exposure to a radiation with dose D and D_0 it is a dose that gives to an average of one hit per cell. The equation 5 describes this probability:

$$P_{hits}(0, D) = e^{-\frac{D}{D_0}} \tag{5}$$

However, the probability to kill cells depends on the type of the radiation. If there are high charged particles, the energy deposition is more than the ionizing radiation like electrons of photons. This is defined with the quantity called linear energy transfer (LET) of a radiation, it is the energy filed per unit length. The LET rage comes from 0.2 keV μm^{-1} for electrons and photons, to rate between 2 and 20 keV μm^{-1} for protons, and for heavier particles it is around 100 keV μm^{-1} [7].

Another important quantity is the relative biological effectiveness (RBE), defined as a radiation capacity, for the same absorbed dose, to induce the same biological effects compared to a reference radiation. The ratio between photons dose and protons dose which gives 10% survival represents the RBE, it is in the equation 6 [7].

$$RBE = \frac{D_{\gamma}^{10}}{D_{p}^{10}} \tag{6}$$

Chapter 2

2 Radioembolization

2.1 Introduction

In nuclear medicine, trans-arterial radioembolization (TARE) is a selective internal radiation therapy (SIRT), which is applied to primary and secondary liver tumours [8]. Primary liver cancer is the fifth most common cancer and the second most frequent cause of cancer-related death globally, accounting for 7% of all cancers. Hepatocellular carcinoma (HCC) represents about 90% of primary liver cancers and constitutes a major global health problem. The major risk factors for liver cancer are hepatitis B and C, chronic consumption of alcohol. There are different stages of this tumour, furthermore it is useful to apply radioembolization for the unresectable one [3]. The tumour phases are classified in five stages from Barcelona-Clinic Liver Cancer (BCLC): 0, A, B, C and D [9]. Very early HCC (stage 0) is defined with a single tumour smaller than 2 cm in diameter, without vasculature invasion [9]. Early HCC (stage A in BCLC) means that the tumour is single and with diameter bigger than 2 or if there are three nodules smaller than 3 cm in diameter [9]. Early-stage liver cancer patients can have different treatments such as resection, liver transplantation or ablation [9]. The intermediate patients (stage B) can benefit intra-arterial treatments such as trans-arterial chemoembolization (TACE) or trans-arterial radioembolization or external beam radiation therapy (EBRT) [9]. Instead, in the advanced stages such as C and D, it is indicated to administer Sorafenib with systemic therapy [9]. The BCLC staging system is shown in figure 2 [9].

Yttrium-90 microspheres are biocompatible but not biodegradable and are introduced, with a catheter, in the patient trough the hepatic artery and these follow the blood flow since the lesions is predominantly vascularized by the artery, while the healthy liver is primarily fed by the portal vein. Preliminary, before treatment it is necessary to perform a computed tomography (CT), an angiography, and a single photon emission computed tomography (SPECT) by ^{99m}Tc-MAA (Macroaggregates of albumin) to evaluate tumour mass, to predict the distribution of the treatment and perform dosimetric planning respectively. Post-treatment, imaging is necessary to verify the microspheres distribution

and the delivered dose to the target. The different steps of radioembolization are mentioned in the figure 3 [8].

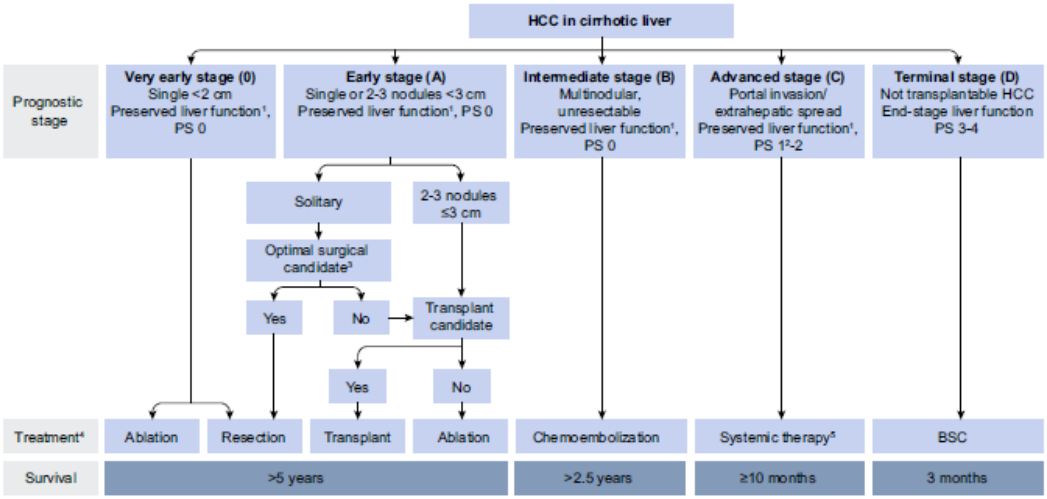

Figure 2 Tumour stages and ways for treatment [9].

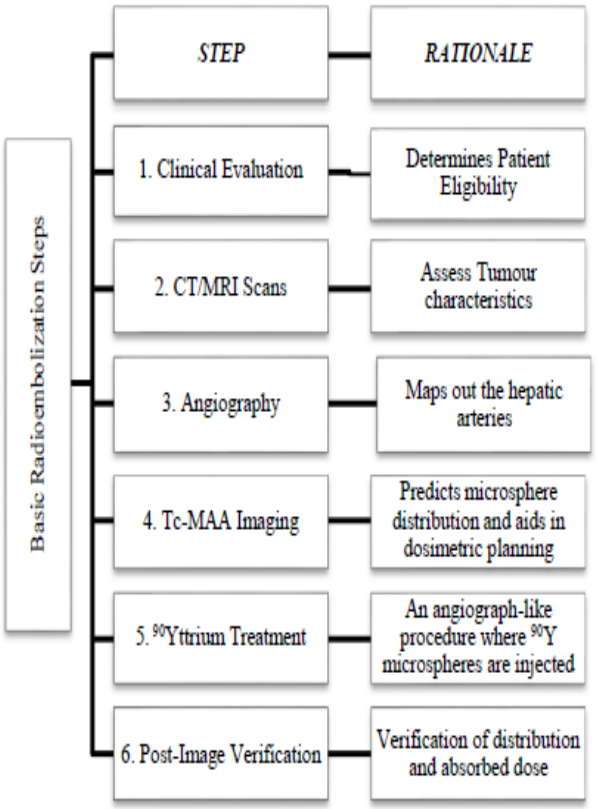

Figure 3 Radioembolization stages [8]

2.2 Yttrium-90 ^{90}Y

Yttrium-90 is an element that does not exist naturally, it is an isotope of yttrium-89. The Yttrium has atomic number 39, it is a transition metal such as gold and silver and it is a rare earth element [10]. Yttrium-89 is not found free in nature, but it is combined with lanthanide elements in rare earth minerals, and it is found in the earth crust [10]. Yttrium-90 is a pure β- emitting radionuclide that is employed in medical applications due to its physical half-life (~64 hours) that becomes stable zirconium ^{90}Zr. The maximum decay energy is 2.28 MeV, and the average energy is 0.937 MeV, with strong penetration in tissues (11 mm), the mean penetration is 2.5 mm [11].

This isotope is selected for radiotherapy since it releases high energy particles that can kill the cancer cells and it departs a small fraction of energy to healthy tissues. In a β- decay it is emitted an electron with high energy, and it occurs the conversion of a neutron in a proton [11]. Yttrium-90 it is considered as a β- emitter, but a small branch of this radionuclide decays into the 0^+ excited state with ^{90}Zr (1.76 MeV). Subsequently, there is an emission of β-/ β+ with a small branching ratio. In the figure 4 is shown the decay of yttrium-90 [12]. The pair production is employed to find the biodistribution of yttrium-90, using positron emission tomography (PET) [13].

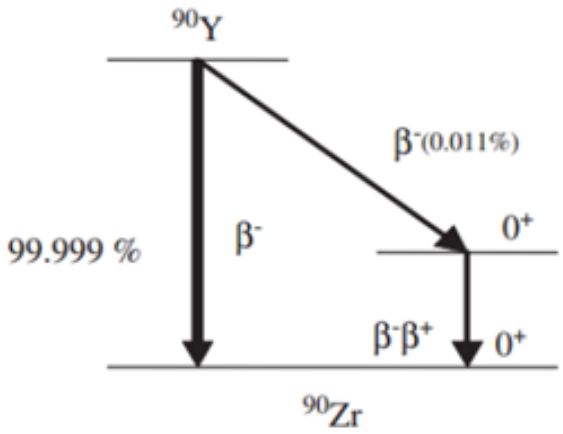

Figure 4 Yttrium-90 decay [12]

It is performed with a minor branch of created positron and electron pair every 32 in one million decays [8]. PET scan can detect the emitted positrons because the high activity of yttrium-90 is deposited in a small region (the liver), therefore the number of positrons is

sufficient to be discovered [13]. The β- particles have dimensions as compared to cells. An important property of these particles is the "crossfire" effect, which guarantees enough dose to each cell in the tissue [11]. Yttrium-90 can be produced in a nuclear reactor by neutron bombardment that transforms the inactive ^{89}Y into radioactive ^{90}Y, without use of an enriched isotope indeed yttrium is mononuclidic [11]. The purity of the isotope depends on the reactor epithermal flux [11]. Another way to produce^{90}Y, in vivo utilizations, it is from ^{90}Sr which is wasted from the fission of uranium in a nuclear power plant by synthesise. In figure 5 it is shown a scheme of ^{90}Sr decay [14]. In medical applications it is fundamental to separate the two ions, yttrium-90 and strontium-90, because the second has similar characteristics of calcium. The sedimentation of strontium-90 can cause leukaemia and bone cancers [11]. Yttrium-90 linked to a specific vector is considerably used in Nuclear Medicine to treat tumours both for systemic and locoregional treatment.

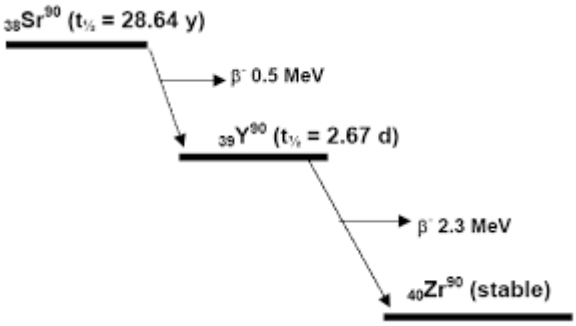

Figure 5 Strontium-90 decay [14]

2.2.1 Yttrium-90 radiopharmaceutical application

The development of cancer treatment is supported by the IAEA, promoting new radionuclide therapies using ionizing radiation in nuclear medicine [15]. The effectiveness radiation dose depends on the radionuclide type and its characteristics, but also it depends on the pharmacodynamic and pharmacokinetic properties of the radiolabelled targeting vehicle [15]. It is noticed that to treat larger tumours effectively should be chosen radionuclides with long range beta emission, such as yttrium-90.

The most widely application of yttrium-90 it is to treat the liver cancer (HCC hepatocellular carcinoma). During these past decades, ^{90}Y-TARE is classified as a safe

and useful treatment for unresectable primary and secondary tumours, but it is also possible to regress the tumour stage.

So, liver tumour is treated with yttrium-90 microspheres with trans-arterial radioembolization (^{90}Y -TARE). There are two types of microspheres: resin microspheres (SIR-Spheres®; SIRTeX Medical, Lane Cove, NSW, Australia) and glass microspheres (TheraSphere®; Nordion, Ottawa, Ontario, Canada). There are differences between these two available types, the more relevant about dimensions, number of spheres in the vial and specific activity. Firstly, the resin microspheres have a diameter of 20 and 60 μm and the spheres per vial are about 40-80 million with single sphere activity of 40-70 Bq per sphere. The size of glass microspheres is 20-30 μm and the spheres per vial is 1.2-8 million with single sphere activity 2500 Bq per sphere [11]. This means that with 1 GBq of resin spheres more particles are infused than the glass spheres, thus leading to a potential embolic effect. Therasphere is injected in 0,6 ml of sterile water, SIR-sphere is supplied in 5 ml of sterile water. It is possible to understand the differences between glass and resin spheres in table 3 [16].

Characteristics	SIR-Spheres®	TheraSphere®
Material	Resin	Glass
Particle size (μm)	20–60	20–30
Number of spheres per vial (range in million)	40–80	1.2–8
Specific gravity	Low	High
Embolic effect	Moderate	Mild
Activity per sphere (Bq)	40–70	2,500
Activity available (GBq)	3	3, 5, 7, 10, 15, 20
Handling for dispensing	Required	Not required
Splitting one vial for two or more patients	Possible	Not possible
Delivery route	Transcatheter, intra-arterial (hepatic) Hepatic ports (rare)	Transcatheter, intra-arterial (hepatic)

Table 3 Comparison of microspheres [6]

Throughout the first 11 days, the 94% dose is released by the microspheres. 1 GBq of ^{90}Y distributed in 1 kg of tissue delivers a total dose of 50 Gy/kg in tissue [17]. The dose absorbed by liver must be between 80 and 150 Gy, which depends on the tumour mass.

2.3 Liver vascularization

The liver is the biggest gland in the human body, that is formed by two lobes, the right lobe, and the left lobe. A liver scheme is reported in figure 6 [18].

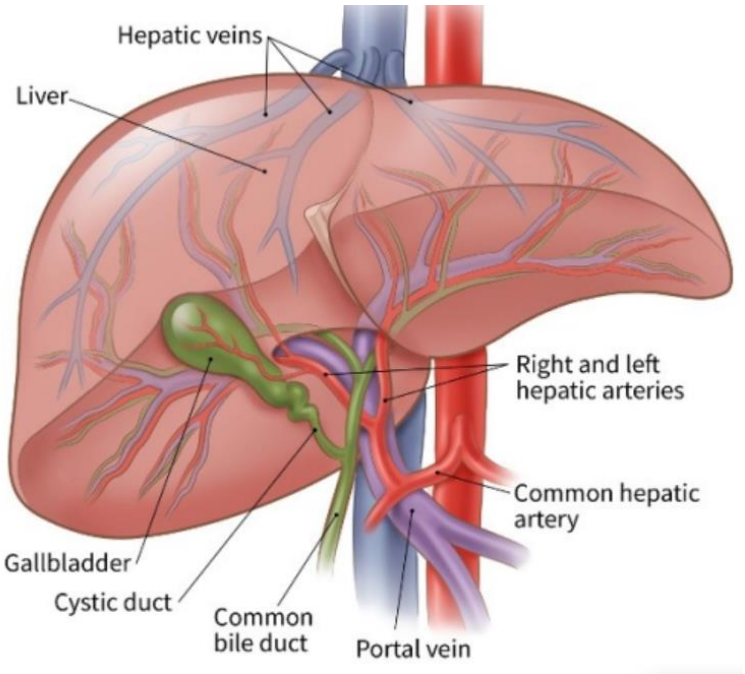

Figure 6 Liver scheme [18]

The gland is in the upper abdomen on the right, under the diaphragm near to the stomach. The liver dimensions are the vertical length 15-17 cm, the horizontal length 20-23 cm, and the weight 1-1,5 kg [19].

The liver has two sides: the upper diaphragmatic surface and the bottom visceral surface [19]. There are different liver functions: the digestion, the organism protection, and the toxic substances elimination. The liver blood supplies are two, the portal vein, that provides 75-80% of the total hepatic blood supply and the hepatic artery, which delivers 20-25% of blood. The hepatic arteries supply the oxygenated blood while the portal vein provides partly deoxygenated blood, but it is rich in nutrients. The portal vein is divided in two branches which pass through the liver lobules. One of the liver functional units is the hepatic lobule, which has a hexagonal structure. The lobules are small (1-2.5 mm), each of them has a central vein, which is surrounded by 6 vessels [19]. The vessels are constituted by a branch of hepatic artery and a branch of portal vein. The capillaries (sinusoids) allow the blood flow from the portal vein and the hepatic artery to the central

vein. Another duct is for the accumulation of the hepatic bile and for the discharge out of the liver. The hepatic lobule scheme is in figure 7 [19].

The liver parenchyma is constituted by hepatocytes, which are cells with a cubic shape with sides equal to 20-30 μm. Hepatocytes are liver cells that perform all the liver functions. The tumour is generated by hepatocytes.

Other important cells in the liver are Kupffer cells, which are called macrophages or phagocytes. The assignment for these cells is to remove the bacterial in the blood flow and to stimulate the replacement of worn cells. Moreover, the Kupffer cells live around 3.8 days, with a proliferative capacity. The Kupffer cells activate if there are hepatic lesions caused by ethanol.

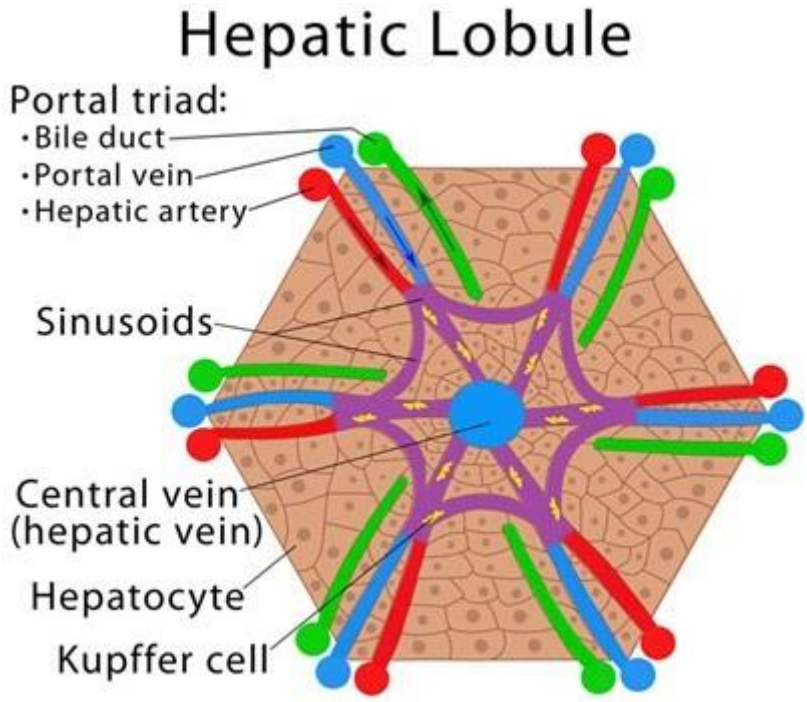

Figure 7 Hepatic lobule [19]

In the liver functional units there are the bile ducts, which formed the biliary tree. The bile produced in the liver moves around in the right and left hepatic duct, and it is deposited in the gallbladder. Lastly the bile goes out to the liver through the common bile duct, which opens into the duodenum [19]. In the figure 8 there is shown the biliary tree [19].

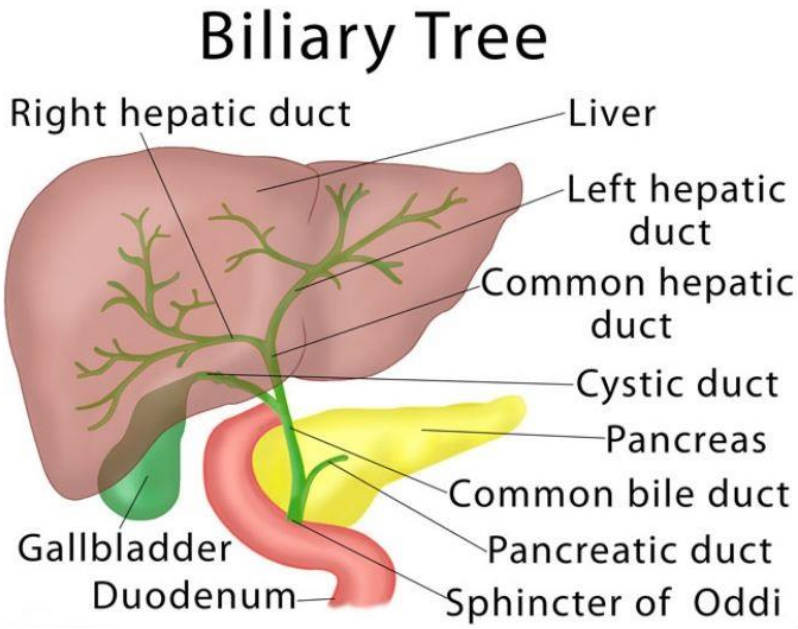

Figure 8 Biliary tree

Normal liver cells are predominantly provided by the portal vein, despite the cancer cells are primarily fed by hepatic artery. Therefore, the microspheres are injected in the hepatic artery. For personalize treatment, it is relevant to predict the spheres distribution to understand the dose delivered on the tissues and to verify the therapy effectiveness. Hepatic microcirculation starts when the right or the left hepatic arteries are split into small arterioles with diameter 50-100 μm, terminal arterioles with diameter 15-50 μm, and finally reach the capillary network with diameter 5-10 μm [8]. The spheres can be localized uniformly in the terminal arterioles of normal tissue and of the lesion. To analyse the spheres' location computational fluid dynamic method (CFD) is used [20]. The analysis is driven to optimize the injection for maximize the tumour targeting. Since the blood flow is influenced by boundary conditions, there should be investigated the physiological conditions and factors with CFD, which influence these conditions. The drug is introduced in the patient with a catheter, and this generates a perturbation on the flow field characteristics, such as blood pressure and blood velocity. In addition, when the tumour growths, the vasculature structure changes near to the lesion, and it implies a variation of the normal liver vasculature. Therefore, it is probable that the microspheres are located also in the healthy parenchyma. Even thought, the analysis is made assuming a homogeneous distribution of spheres in the liver. For the simulation there are employed three-dimensional Navier-Stokes's mass conservation (equation 7) and momentum

equations (equation 8) for laminar incompressible flow to estimate flow field in the domain [20].

$$\nabla \cdot (\rho u) = 0 \tag{7}$$

$$\rho\left(\frac{\partial u}{\partial t} + u \cdot \nabla u\right) = -\nabla p + \mu \nabla^2 u + \frac{1}{3}\mu \nabla(\nabla \cdot u) \tag{8}$$

Where u is the flow velocity, p is the flow pressure, ρ and μ are the blood density and the dynamic viscosity of blood. Since the cancer cells are fed by hepatic artery, which is a large artery with diameter greater than one millimetre, for the blood behaviour it is assumed a Newtonian model [20]. The blood is compared to an incompressible fluid with density 1.06 gr/cm^3 and with dynamic viscosity 0.04 gr/cms [20]. Another assumption is that the flow is laminar, so the Reynolds number is calculated, and it is below the laminar-turbulent transition limit (2300<Re<4000) in every situation [20].

Instead of what the previous analysis demonstrated, in the reality, the distribution of the microspheres is not homogenous but heterogeneous, as it is illustrated in multiple studies [8]. This means that the absorbed dose is not uniformly spread. A predominant part of the radiation emitted by microspheres is absorbed near the source location, and it has been shown that less of 1% of normal tissue absorbs more than 30 Gy [8]. Although from different studies it is demonstrated that both resin and glass microspheres are similarly dispersed inside the tumour nodules.

2.4 Pre-treatment procedures

The preliminary step is the pre-treatment. With angiography and single photon emission computed tomography (SPECT), before the treatment, the vascularization of the patient is analysed, and the distribution of the microspheres is simulated.

2.4.1 Angiography

In the first phase it is made an angiography of the hepatic vascularization to identify all the possible anatomical variants and all possible subsidiary branches of neoplastic lesions, and arterial departments of extra-hepatic relevance, such as the gastroduodenal, the

gastric, and the pyloric small arteries. Another aim of the angiography is to guide the delivery catheter positioning, as well as to evaluate blood flow and to estimate the extrahepatic microspheres deposition [8]. Once the angiography is done, it is recommended coil embolization of possible variant vessels. A catheter and a metal cable, which has attached collagen fibres, are used for embolization. The metal cable is a spiral and it is released in the aberrant vessels to occlude them to avoid delivering the spheres outside the target lesion. The collagen fibres attach the vessel, and induce thrombosis, which blocks the blood flow in the vessel and the microspheres transit. This process ensures the microsphere insertion directly in the targeted region. An example of angiography imaging is shown in figure 9 [8].

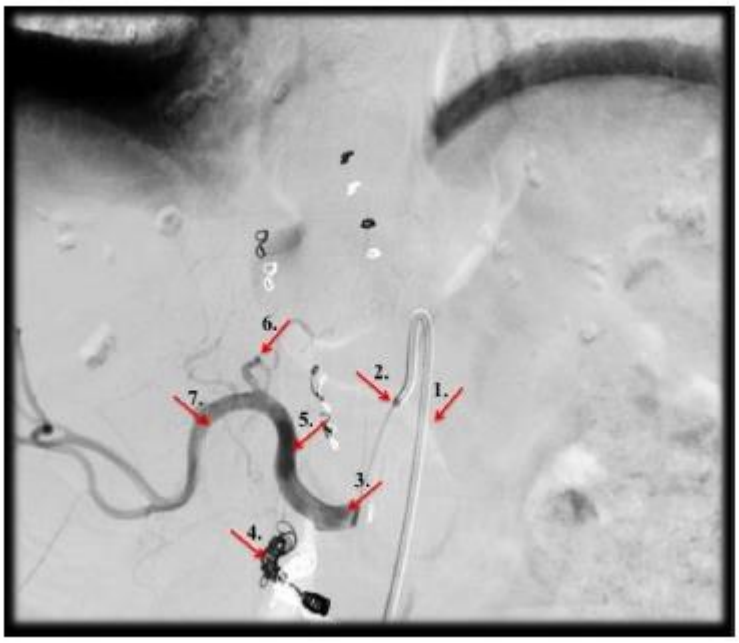

Figure 9 Here it is represented a right lobe embolization. The different sections of the hepatic vessels are: 1. Catheter in the celiac truck, 2. Micro-catheter which is extended to 3. The hepatic artery, 4. A gastroduodenal artery with coil embolization, 5. Proper hepatic artery, 6. Left hepatic artery. 7. Right hepatic artery [8].

Angiography session is performed endo-arterial administration of contrast using anendo-arterial catheter, to analyse the blood vessels. The catheter is a slender plastic tube which is inserted in the patient artery through an incision in the skin [21]. Furthermore, the catheter usage has a dual feature, the imaging guide, and the injection of the contrast material.

The outcome pictures are used to diagnose and treat blood vessel illness and it is possible to take them using [21]:

- X-rays
- Computed tomography
- Magnetic resonance imaging.

The examination is made with a radiographic table, an x-ray tubes and a monitor [21]. In the figure 10 [22] there is shown the angiography room. The conversion of x-rays into images is made with fluoroscopy, which is a guide for the procedures [21].

There are followed several steps to perform the exam. Firstly, there is made a small cut in the interested area. The catheter passes through this incision, and it reaches the right position for the examination. Afterwards the contrast material is injected in the tube, and it arrives at the blood vessels, then x-rays are taken. The procedure lasts approximately an hour [21]. In the end the catheter is removed, and the incision is closed.

Figure 10 Angiography room [22]

2.4.2 ^{99m}Tc-MAA SPECT/CT

^{99m}Tc-MAA (Macroaggregates of albumin) SPECT/CT imaging is fundamental to predict the microspheres distribution, and to establish the activity that is necessary to treat the tumour. Another important benefit of this examination is related to the quantification of possible lung shunt fractions and gastrointestinal shunts. Before doing the therapy, it is mandatory to verify the patient eligibility, to assess the lung shunt fraction (LSF), to assess the uptake in tumoral and normal tissues, and to exclude gastrointestinal shunts.

^{99}Tc occurs naturally in a small part of the earth's crust, for this reason, this isotope is produced artificially from molybdenum or by extraction from nuclear chain reaction, as a product of uranium and plutonium. There are two types of technetium: ^{99m}Tc where m means metastable, that has shorter life than ^{99}Tc and there is ^{99}Tc. Since the shorter life of a metastable isotope, in medical application it is convenient to use ^{99m}Tc. The molybdenum-99 is shipped to the hospital, which has a short half-life about 2,75 days, and from its decay it is generated technetium-99 metastable. During the ^{99m}Tc decay gamma-rays emission occurs with a photon energy of 140 Kev and its half-life is 6 hours. After 24 hours the metastable technetium becomes ^{99}Tc. The ^{99m}Tc administration to the patient is provided by a vial of 10 ml solution with $4.8x10^6$ aggregated albumin particles, which have diameter between 10 and 90 μm [8]. Therefore, due to the short half-life of ^{99m}Tc, and to assess the realistic MAA distribution, the imaging must be done at least within 60 minutes after the administration. Preliminary therapy session is simulated with ^{99m}Tc by trans-arterial injection. After injection whole-body gamma camera detection system is performed in the Nuclear Medicine Division. For an accurate evaluation of the microspheres' distribution, is routinely used SPECT/CT system. This is better than planar imaging to assess if there is extrahepatic deposition or non-homogeneous deposition of the radiopharmaceutical. The forecast is significant to find the exact activity that should be administered to the tumour by limiting extrahepatic exposure. There are differences between ^{99m}Tc-MAA and ^{90}Y microspheres features: these have different size, radioactivity, and density. The ^{99m}Tc-MAA accumulation is mainly axial and large particles of technetium-MAA deposit in vessels of high flow while small particles are deflected to vessels with lower flow [8]. So, this implies that the ^{99m}Tc-MAA has high heterogeneity distribution with respect to ^{90}Y microspheres [8].

"HCC is characterized by arteriovenous shunting bypassing the capillary bed. In the case of arteriovenous shunt, both lungs are uniformly perfused through the vena cava, heart and lung arteries" [11]. Lung shunting can result in radiation pneumonitis after treatment administration. Therefore, before the treatment it is mandatory to quantify the lung shunt fraction (LSF) and if the value is high the patient is not eligible for the cure. Considering injected activity of 75-150 MBq of ^{99m}Tc-MAA in the hepatic artery through the catheter the lung shunt fraction (LSF) is evaluated with the equation 9 [16].

$$Lung\ shunt\ fraction = \frac{lung\ counts}{lung + liver\ counts} \tag{9}$$

For the resin spheres three methods are available to evaluate the dose: the empiric, the body surface area and the partitional method. The first method considers the percent tumour contribution on the total liver to find the proper activity. The research is made with CT and MRI to find the dimensions of the tumour and the liver, and the method considers the lung shunt fraction. However, this approach is forsaken because the safety margin to reduce side effects is low. In the table 4 is represented this method [8].

Prescribed Dose Based on Tumour Load.

Resin		Reduced Load for Resin based on Lung Shunt	
		Lung Shunt Percentage	Activity of Spheres
Empiric Method	> 50% Tumour Load = 3 GBq	< 10%	Full prescribed activity
	25–50% Tumour Load = 2.5 GBq	10–15%	Reduce activity by 20%
	< 25% Tumour Load = 2 GBq	15–20%	Reduce activity by 40%
		> 20%	Do not give SIR-Spheres

Table 4

The patients with lung shunt fraction higher than 20% of the total injected dose or with a lung dose higher than 30 Gy for a lung mass of 1 kg should be excluded from the treatment. It is mandatory to consider the lung shunt fraction for the calculation of the total activity injected. After the administration, a SPECT/CT is acquired within 120 minutes. In SPECT one or more large detectors with a diameter of 50 cm, rotate around the patient, and only the direct photons which are perpendicular to the detector are spotted. SPECT is performed to study the distribution of radioactive compound in internal

organs. The exam is performed by a gamma camera that reveals the isotope distribution in the body, and it is used for diagnostic and therapeutic purposes.

This device comprises a collimator and a gamma-rays detector. The radiation pass through the tissues and reaches the detector. Usually, SPECT imaging is associated with a computed tomography (CT) imaging (SPECT/CT), that is acquired after SPECT acquisition to perform the registration of functional with anatomical imaging.

2.5 Dosimetric methods

Different dosimetric methods are proposed to quantify the activity to deliver to the tumour. Radioembolization employs the MIRD formalism, which translate activity in Bq to absorbed dose in Gy [8]. Three methods are proposed by resin microspheres manufactures: the empirical method that is based only on tumour volume (the larger the tumour burden, the higher the recommended activity), the body surface area (BSA) method that incorporates also body surface area, assuming a correlation between BSA and tumour volume, and the multi-compartmental Medical Internal Radiation Dose (MIRD) macro dosimetry or partition model, that hypnotizes that the three compartments involved in radioembolization are distinguishable between them. For glass spheres only mono-compartmental MIRD macro dosimetry method is proposed, that is slightly simplified, assuming homogeneous activity distribution in the liver, tumour and lung (if any shunting occurs).

The quantity of ^{90}Y microspheres is calibrated in activity (GBq), although the doses of radiation therapy are planned in Gy (J/kg) to estimate the fraction of absorbed dose in tissue. Furthermore, in radioembolization the prescribed dose is planned in Gy, but it is needed to convert the dosage before treatment in activity. The administered activity is not always the same as the prescribed activity.

For the calculation of the absorbed dose the MIRD (Medical Internal Radiation Dose) which provides a systematic approach to blending the biologic distribution data and the characteristics of radionuclides to find dose estimates is preferably used [9]. Radioembolization applies the MIRD formalism and converts activity to absorbed dose in Gy [8]. The equation 10 [8] is for the simplest case where all the activity is deposited in the perfused liver volume.

$$D[Gy] = 50\left[\frac{J}{GBq}\right] \cdot \left(\frac{A[GBq]}{m[kg]}\right) \tag{10}$$

In the previous equation, the administered activity is converted to absorbed dose, considering that 1 GBq of administered activity per kg of tissue mass supplies an absorbed dose of 50 Gy [8]. An assumption underlying this conversion is based on the uniformly yttrium distribution in the tumorous tissue and healthy hepatic parenchyma to provide a uniform distribution of dose. A CT scan serves to quantify the liver volume which multiplied for its density in g/cm^3 gives the mass. Moreover, must be considered the lung shunt fraction to discover the needed activity because extrahepatic deposition leads to an yttrium sedimentation in the lung volume and not only in the liver volume. The partitioned dose in the lung is quantified by the equation 11 [8].

$$D_{lung}[Gy] = 50\left[\frac{J}{GBq}\right] \cdot \left(\frac{A_{total}[GBq]}{m_{lung}[kg]}\right) \cdot LSF \tag{11}$$

For evaluate the total activity (A_{total}), which is the sum of the activity in the liver and the activity in the lung, there are the equation 12, the equation 13 and 14 [8].

$$A_{total}[GBq] = A_{lung} + A_{liver} \tag{12}$$

$$A_{liver}[GBq] = A_{total} \cdot (1 - LSF) \tag{13}$$

$$A_{lung}[GBq] = A_{total} \cdot LSF \tag{14}$$

The calculation of LSF is given in the table 5, which is suggested by the manufacturer [8].

Description for Calculation of LSF.

LSF Calculation	$LSF = \frac{counts_{lung}}{counts_{lung} + counts_{liver}} \times 100$ for lung shunt percentage	
SIR-Sphere (Resin) [4]	LSF	Activity Given
	> 20%	No Activity
	15%–20%	Reduce by 40%
	10%–15%	Reduce by 20%
	< 10%	Give full amount of activity
TheraSphere (Glass) [3]	Upper Lung Shunt Activity Limit: LSF [%] × A[GBq] = 0.61 GBq A[GBq] = Activity prescribed during pre-treatment dosimetry	

These calculations are recommended based on planar scintigraphic imaging, but SPECT/CT derived data is much more reliable.

Table 5

The method introduced after the empiric method is the body surface area (BSA), which correlates the BSA with the size of whole liver of the patient. The prescribed activity can be fixed without the liver volumetry on cross-sectional imaging [8]. Also, in this approach there is considered the lung shunt fraction and the scheduled activity is calculated with equations 15 and 16 [8].

$$A[GBq] = (BSA - 0.2) + \left(\frac{tumour\ volume}{tumour\ volume + liver\ volume}\right) \quad (15)$$

$$BSA = 0.20247 \cdot height[m]^{0.725} \cdot weight[kg]^{0.425} \quad (16)$$

The tumour and the liver volume are found with CT and MRI scans. It is noticed with this method that there is an overdose of small liver and an underdose of large liver. Another limitation is related to the neglect of the tumour-to-normal liver ratio (T/N) from Tc-MAA image, and the limit of injected activity is from 1 to 3 Gy. The tumour-to-normal liver ratio is shown in equation 17 [8].

$$\frac{T}{N} = (A_{tumour}/m_{tumour})/\ (A_{normal\ liver}/m_{normal\ liver}) \quad (17)$$

This ratio can be found by the distribution of ^{99m}Tc, in the preliminary administration, in the tumour and in the normal tissue. The most precise approach, which is only used for the resin spheres, is the partitioned model [8]. This method analyses the perfused liver in tumour and normal volumes, including the lung shunt fraction [8]. The masses of the compartments are discovered by CT and MRI scans [8]. However, the lung shunt fraction is evaluated with the injection of ^{99m}Tc-MAA and it is detected with SPECT/CT [8]. Also, with technetium distribution it is detected the tumour-to-normal liver ratio, the equation

is the same of the BSA method [8]. This allows to prescribe an activity that has a limit related to the maximum dose acceptable to normal liver tissue and it is in equation 18 [8].

$$A[GBq] = \frac{D[Gy] \cdot \left(\frac{T}{N} \cdot m_{tumour}[kg] + m_{normal}[kg]\right)}{50\left[\frac{J}{GBq}\right] \cdot (1 - LSF)} \tag{18}$$

$$D[Gy] = maximum\ Dose\ for\ Perfused\ Normal\ Liver$$

$$A[GBq] = Total\ Prescribed\ Activity$$

Considering the liver partitions, it is possible to find the absorbed dose of the normal liver and tumour with the equations 19 and 20 [8].

$$D_{normal}[Gy] = \frac{50\ \left[\frac{J}{GBq}\right] \cdot (A_{total})[GBq](1 - LSF)}{m_{normal}[kg] + \left(\frac{T}{N}\right)(m_{tumour})[kg]} \tag{19}$$

$$D_{tumour}[Gy] = \frac{T}{N} \cdot D_{normal} \tag{20}$$

The ^{99m}Tc-MAA distribution in normal and tumour liver serves to identify the region of interest (ROIs) to find the counts ratio [8]. Counts is proportional to the activity, therefor the activity ratio is comparable to the count ratio. The total administered activity is in the equation 21 [8].

$$A_{total}[GBq] = A_{normal} + A_{tumour} + A_{lung} \tag{21}$$

The ROIs examined are the partitioned volumes, which are the tumour volume inside the liver, normal liver, and lung.

For the glass microspheres there is only one available dosimetric method called mono-compartmental method. Assuming that for 1 GBq per kilogram of tissue mass compared with 50 Gy and it is in the equation 22 [8].

$$A[GBq] = \frac{D[Gy] \cdot m_{liver}[kg]}{50\left[\frac{J}{GBq}\right] \cdot (1 - LSF)} \tag{22}$$

$$D[Gy] = Prescribed\ Dose\ of\ Perfused\ Liver$$

With the mono-compartmental method it is considered only the total perfused liver volume avoiding the liver partitions. In this procedure the overestimation of the absorbed dose is not present during the conversion from the activity [8].

The absorbed dose of glass spheres is taken from MIRD, on the other hand for the resin spheres this method includes both the prescribed and the administered activity, it can be seen in the equation 23 [8].

$$D[Gy] = \frac{50\left[\frac{J}{GBq}\right] \cdot A[GBq\ of\ administered\ activity] \cdot (1 - LSF)}{m_{liver}[kg]} \tag{23}$$

$$D[Gy] = administered\ Dose\ of\ Perfused\ Liver$$

The dosimetric methods analysed previously have some limitations. First, the microspheres' distribution is not uniformly but heterogeneous in tumour and non-tumour tissue. The heterogeneity of the distribution is driven by the micro-vasculature, and it causes the variation of the absorbed dose in the region of interest. Furthermore, with these methods it is not considered the long beta particle range. The partition method delimits the regions of the liver between tumour and non-tumour areas. Due to the long range of beta particles, it is possible to have the "crossfire" effect. This phenomenon is related to the deposition of particles emitted from ^{90}Y in a non-targeted region from the neighbourhood targeted region.

2.6 Treatment

After the preliminary session with the angiography and the injection of ^{99m}Tc-MAA to identify the distribution of the microspheres, the collected data are sent to the pharmaceutically company. To receive the vial in the hospital it is necessary to let pass at

least one week. After two weeks the vascularization of the patient, which was detected with the preliminary angiography, can change and for this reason must not let it pass more than two weeks between pre-therapeutic evaluation and treatment for the administration of microspheres. Ones that the vial arrives in the hospital it is sent in the Nuclear Medicine Department with complete administration kit and the injection is made in the operating room with a catheter, which is connected to the kit. In the figure 11 it is shown the glass box [23]. The Nuclear Medicine Physician cannot inject the microspheres by hands due to the contamination and the radiation. Therefore, the vial is sent from the pharmaceutically company in a shielded container and the only problem is the motion of the kit out of the box. Another source of contamination is the catheter in which it is possible to find some spheres after the injection. Furthermore, all the medical staff needs a check at the exit of the surgery with Geiger-Muller counter to evaluate the contamination during treatment. The injection is performed with a small super selective catheter which is inserted in the hepatic artery.

Figure 11 Radioembolization kit [23]

The radioembolization is carried out with local anaesthesia and with a small incision of the groin. The dimension of the tube is mandatory because the velocity and the pressure of the microspheres' stream should be comparable to the flow in the artery. If the injection flux is higher than the arterial vessel it causes a reflux of the microspheres and a

dispersion of radioactivity in non-targeted areas [8]. The infusion of resin or glass microspheres is the same except for the need to monitor the SIR-sphere in the artery with fluoroscopy. This process is performed due to the high number of resin spheres in the vial which can causes an occlusion of the vessel. For this reason, to ensure fluidity of the stream it is inserted sterile water. The administration of SIR-spheres must be interrupt when the vial is empty or when there is a reflux of spheres in the catheter, and the treatment cannot be ended, it means that there is an incomplete administration of the total prescribed activity [8]. For the Theraspheres it is not required to track the spheres path in the artery because glass spheres do not cause flow stasis. To increase safety margins, it is preferable to treat only one lobe at a time. Moreover, if the patient has a bilobar liver tumour the treatment is performed in two different times, in which it is cure one lobe at a time. After the administration of the spheres, the dose is delivered during the following 11 days [12].

2.7 Post-treatment

After the administration of the microspheres, the next step is to detect the distribution and to estimate activity in the tissues. To detect the ^{90}Y-microspheres activity in the patients a PET/CT scan is performed, or, when not available, a SPECT/CT scan. The injected isotope is ^{90}Y which a pure beta-emitter. Mainly, ^{90}Y produces bremsstrahlung photons with energy spectrum higher than the maximum energy of beta particles [8]. It is not easy to select a proper energy window since the energy spectrum of photons has no photopeak [8]. Another phenomenon that occurs is the photoelectric effect due to the interaction of photons and the patient's tissues, which attenuates photons. There is coherent scattering and Compton scattering which change the original direction of photons. On the other hand, PET/CT has higher spatial resolution and sensitivity. ^{90}Y can create positron and electron pair in a small fraction, only 32 in one million decays. For the PET imaging it is used the annihilation of this positron. Since it is necessary introduce an attenuation correction of different tissues density, the two scans are performed with CT. Early side effects are rare, principally fever and nausea could occur, but these are mild and normal symptoms, however, is important monitoring liver function by blood exam in the first weeks after treatment, instead response to therapy is assessed by radiological evaluation

at least 3 months after treatment. In the figure 12 [17] are shown the pre-treatment imaging with ^{99m}Tc-MAA and the post-treatment imaging with ^{90}Y-microspheres.

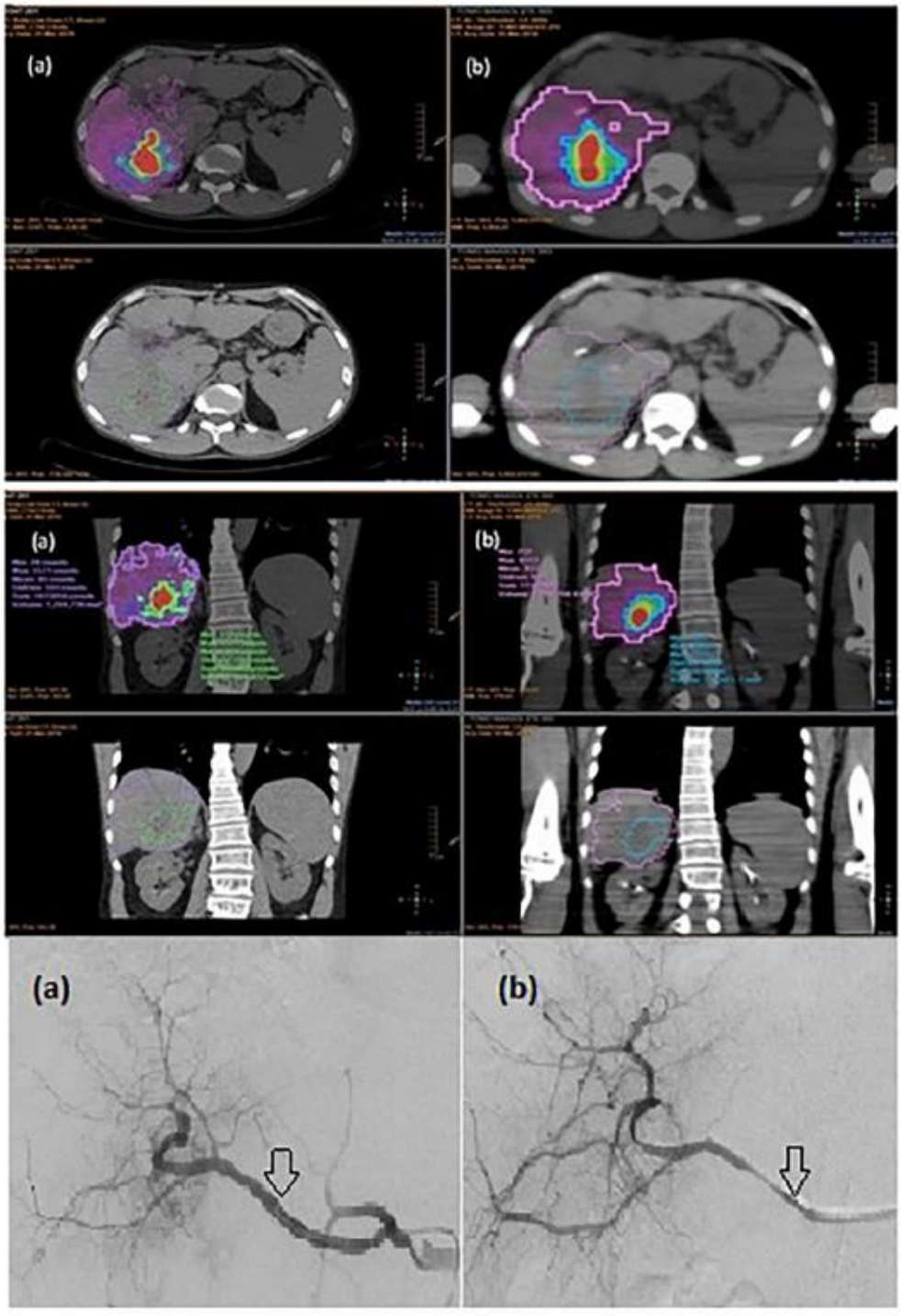

Figure 12 The left side shows the pre-treatment imaging (SPECT/CT); The right side represents the post-treatment imaging (PET/CT) [17].

2.7.1 Positron emission tomography (PET)

PET procedure is started with the radioisotope injection with short half-life. The annihilation is exploited for this examination. After the injection of the isotope in the bloodstream, it decays emitting a positron. The interaction between the positron and the electron generates the annihilation phenomenon. Moreover, the product of this event is a photon pair each emitted with energy equal to 511 keV. The pair is detected by a scintillator and multiplicator tube finds out the bright flash. For the investigation only the photon pair, which reach the detector, are taken into consideration. The detectors recognise which photon comes first, then these can locate the source. The figure 13 [24] represents the procedure to perform PET. The acquisition time is about 15-20 minutes.

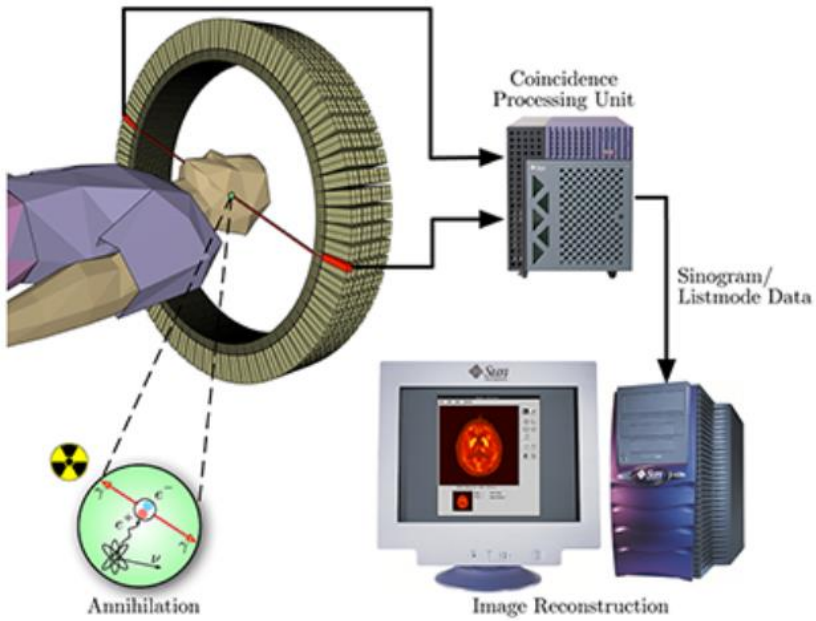

Figure 13 Process to perform PET [24]

PET is coupled with a CT system (PET/CT) has high sensitivity with respect to SPECT/CT and the resolution is better. The positron emission tomography acquisition is 3D, however the capture in SPECT is 2D and it is reconstructed in 3D. Another difference is the type of the tracers which are introduced in the bloodstream [25]. SPECT scan detects direct gamma rays although PET reveals the gamma rays produced by the positron

and electron interaction. For both acquisition modalities the patient is supine, but in PET acquisition the machine does not revolve around.

Chapter 3

3 Material and methods

We retrospectively analysed thirteen patients (Male n° 12 / Female n° 1, median age 64 – range 51-83) treated at Nuclear Medicine Division of AOU Città della Salute e della Scienza di Torino with ^{90}Y TARE with ^{90}Y-glass microspheres (Theraspheres®) for unilobar HCC between June 2019 and April 2021. Median administered activity was 2.3 GBq (1 - 3.5 GBq). Before the treatment, an angiography was performed to map specific arteries of the patient; then, a preliminary simulation was made with injection of ^{99m}Tc-MAA in order to predict the distribution of ^{90}Y-microspheres in the tissues by a total body planar image and an abdomen SPECT/CT acquisition (GE Discovery NM/CT 670) and to perform dosimetric evaluation. The figure 14 shows the SPECT/CT machine [26].

Figure 14 SPECT/CT [26]

Activities to administered were calculated with different methods.

The first method was the multi-compartimental MIRD: there were evaluated two different volumes of interest, one for the tumour and another for the normal liver. In this approach the mean absorbed dose is evaluated in different volumes of interest [27]. In the figure 15 it is reported a tomographic image where there were drawn the interested volumes.

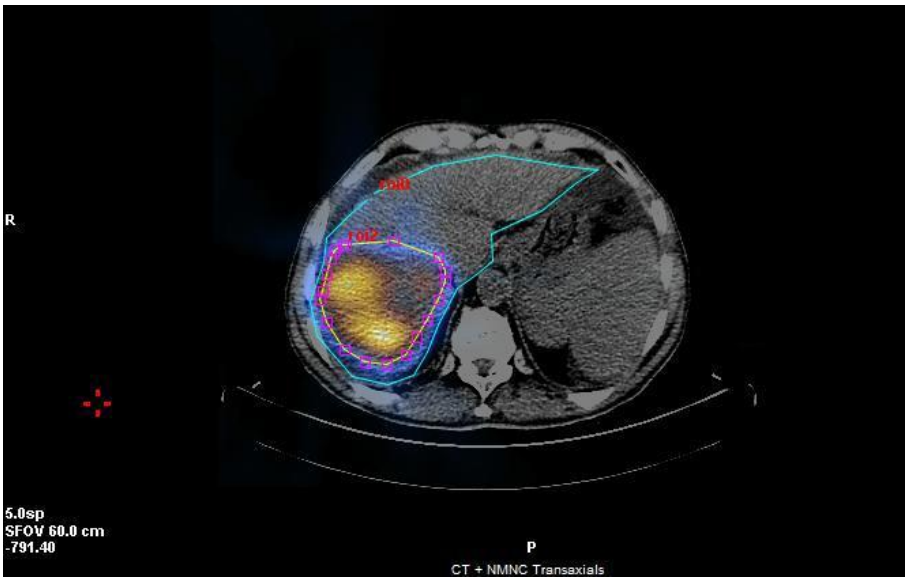

Figure 15 Image of VOIs drawn in tomographic acquisition

Defining the volumes, the masses were evaluated multiplying the volumes by the densities (1.03 g/cm^3). The calculations of this procedure were computed on a MATLAB script for simplicity. The equation 24 was carried out for the evaluation of the dose fraction deposited in the tumour [28].

$$fractional\ uptake_{Tumour} = (1 - L)\left(\frac{(TLR \cdot m_{tumour})}{TLR \cdot m_{tumour} + m_{normal\ liver}}\right) \tag{24}$$

Where L is the lung shunt fraction, which is assumed equal to zero in the script; m_{tumour} is the tumour mass and $m_{normal\ liver}$ is the normal liver mass. In the volume of interest (VOI) evaluation the tumour-to-normal tissue ratio (T/N) is called TLR, but the meaning is the same. The equation 25 was for the calculation of tumour-to-normal tissue ratio.

$$\frac{T}{N} = (Counts_{tumour}/m_{tumour})/(Counts_{normal\ liver}/m_{normal\ liver}) \tag{25}$$

The dose accumulated in the normal liver was found with the equation 26.

$$fractional\ uptake_{Normal\ Liver} = (1 - L)\left(\frac{(m_{Normal\ Liver})}{TLR \cdot m_{tumour} + m_{normal\ liver}}\right) \quad (26)$$

Another two evaluated quantities were the mean dose for tumour and healthy liver, which had the equation 27 and 28 [28].

$$Dose_{tumour}(Gy) = \frac{50(Gy \cdot kg)}{GBq}\frac{(A(GBq) \cdot fractional\ uptake_{Tumour})}{m_{tumour}(kg)} \quad (27)$$

$$Dose_{NormalLiver}(Gy) = \frac{50(Gy \cdot kg)}{GBq}\frac{(A(GBq) \cdot fractional\ uptake_{NormalLiver})}{m_{NormalLiver}(kg)} \quad (28)$$

The second method was the Voxel-based method, which uses the SPECT-CT 3D correction matrix. For this approach it was developed a MATLAB (Mathworks) code by medical physicist in the hospital [17].

This procedure was driven by convolution calculations. For chosen target volume i, the mean absorbed dose D_i was computed as the product between the activity $\tilde{A}_k$ and the S factor. The values of S factor were taken from the online database (http://www.medphys.it/), for glass spheres the voxel size was 3.45 mm [29]. The mean dose D_i was evaluated from N surrounding source voxels in the three axes, which is in the equation 29 [17].

$$D_i = \sum_{k=0}^{N} \tilde{A}_k \cdot S_k \quad (29)$$

Where the absorbed dose to the target per unit of activity which is cumulated in a source voxel was represented by S_k (mGy/MBq·s). The summation starts from 0 to include the contribution of self-irradiation. The cumulated activity was found with the equation 30 [17].

$$\tilde{A}_k = 1.443 \cdot A_k \cdot t_{\frac{1}{2}}(^{90}Y) \quad (30)$$

Where $t_{1/2}$ is the physical half-live of ^{90}Y, which is the time let passes to obtain half decays of the isotope. The A_k is the initial activity that was present in the voxel k and 1.443 is the inverse of the logarithm of 2.

For these two methods it was used only one MATLAB script, which included both the methodology. Afterwards running the code, in the command windows comes out the report with all the needed information for the dosimetric estimation. In the figure 16 there is an example of the outcomes of the program for one patient, where there is a comparison between the first and the second method.

In addition to the report there are graphs. The figure 17 represents two charts, one for the normal liver and one for the lesion, where on the abscissa is reported the absorbed dose (Gy) and on the ordinate is reported the volume of the interest tissue.

The graphs in the figure 18 show the Dose Volume Histogram (DVH) curves. The abscissa represents the dose difference, while the ordinate reports the percentage dose difference. D_{95}, D_{50} and D_5 are the specific dose levels. The dose-volume histogram allows to find how much dose is received by a given fraction of a volume.

```
MATLAB Command Window

ANALISI SPECT

Inserisci il nome del paziente


SELEZIONARE IL FILE .dcm DELLA SPECT

SPECT= le dimensioni della matrice dei conteggi sono    128    128    128
SPECT= numero totale di pixel  2097152

SPECT= le dimensioni del voxel in mm sono 4.4181 4.4181 4.4181
SPECT= volume del voxel in cc 0.0862

SPECT= massimo matrice conteggi     4788

SPECT= inserisci il numero di intervalli per l'istogramma  100
SPECT= inserisci il volume del lobo irradiato (inclusa la lesione) in cc  1382
SPECT= inserisci il volume del fegato totale (inclusa la lesione) in cc  1917
SPECT= inserisci il volume delle lesioni in cc  40


SPECT= volume del LOBO IRRADIATO 1520.2 cc, numero totale conteggi 10492064, soglia↙
0.02
SPECT= volume della LESIONE       39.8 cc, numero totale conteggi  1290573, soglia↙
0.46

SPECT= Dosi al LOBO SANO:   minima    3.1 Gy/GBq, media   28.3 Gy/GBq, massima  120.5↙
Gy/GBq
SPECT= Dosi al FEGATO TOTALE SANO (Volumi Q-metrix):  media   20.2 Gy/GBq
SPECT= Dosi alla LESIONE:     minima  109.2 Gy/GBq, media  143.1 Gy/GBq, massima↙
237.5 Gy/GBq

SPECT= inserisci l'attività somministrata in GBq  1

SPECT= le dosi rilasciate ai volumi risultano
 Dose media al FEGATO TOTALE SANO (Volumi Q-metrix):       media   20.2 Gy
 Dosi al LOBO SANO:       minima    3.1 Gy, media   28.3 Gy, massima  120.5 Gy
 Dosi alla LESIONE:         minima  109.2 Gy, media  143.1 Gy, massima  237.5 Gy



Inserisci il numero di intervalli in cui dividere l'istogramma di dose   100

confronto MIRD-Voxel SPECT

Dose media Voxel Lobo sano    28.27 Gy/GBq
Dose media Voxel Fegato sano    20.22 Gy/GBq
Dose media Voxel lesione   143.06 Gy/GBq
Dose media MIRD Lobo sano    28.94 Gy/GBq
Dose media MIRD Fegato sano    20.69 Gy/GBq
Dose media MIRD lesione   151.14 Gy/GBq

Parametri DVH SPECT

Lobo sano D95     5.60 Gy, D50    16.57 Gy,  D5    90.44 Gy

Lesione D95   116.43 Gy, D50   135.93 Gy, D5   204.14 Gy

Omogeneity Index DVH

DVH Lobo sano SPECT     5.12
DVH Lesione SPECT     0.65
```

Figure 16 MATLAB outcome

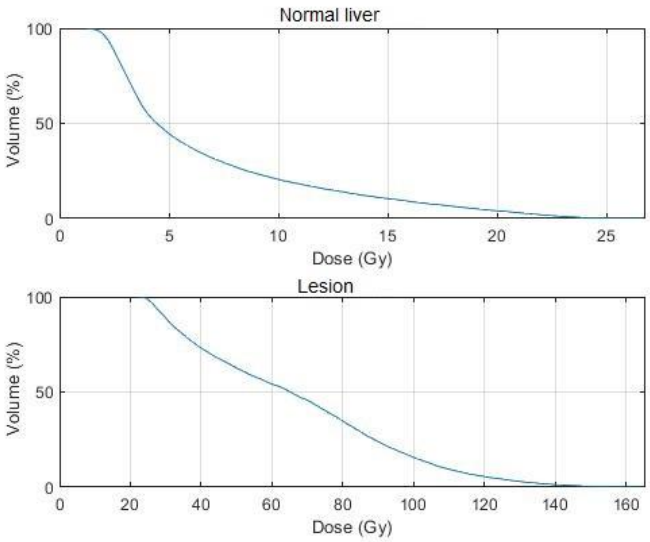

Figure 17

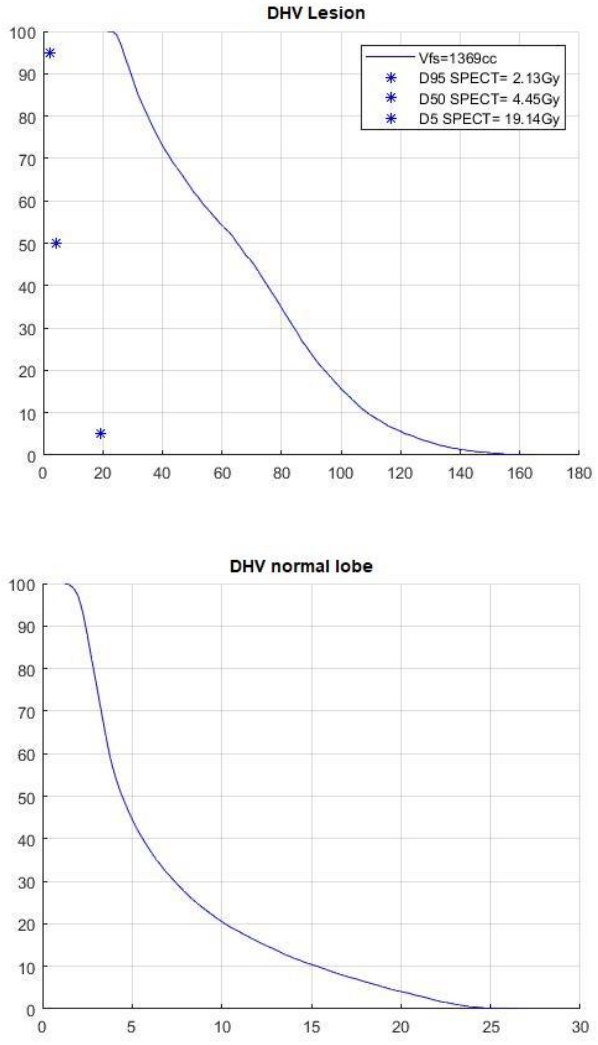

Figure 18

The third and the last method for the dosimetric calculation was performed by Simplicity90Y, which is not an opensource software dedicate to dosimetric planning and assessing image data for general clinical diagnostic. The intended use of this software is analysed medical images, to display data and to help the operators to manipulate images. Dosimetric estimation can be performed with one-compartment, multi-compartment, and voxel-wise techniques [30]. Simplicity can support different types of data [31]:

• CT

• MR

• NM

• SPECT

• PET.

The following image types are supported by the software [31]:

• Multiphase CT

• Cone beam CT

• Multiphase MR

• Planar NM

• 99mTc-MAA SPECT/CT

• FDG PET/CT

• ^{90}Y PET/CT (post-treatment only)

• ^{90}Y SPECT/CT (post-treatment only).

After images acquisition of the patient, the contour of the liver and the tumoral areas on the SPECT image have been drawn. Another important point is related to the calculation of the lung shunt fraction performed from planar image. It is also possible to introduce manually the lung shunt fraction. After all, the extrapolates the absorbed dose by the liver normal tissue and by the tumour. In the following figures 19, 20 and 21 is illustrated the Simplicity report for a single patient.

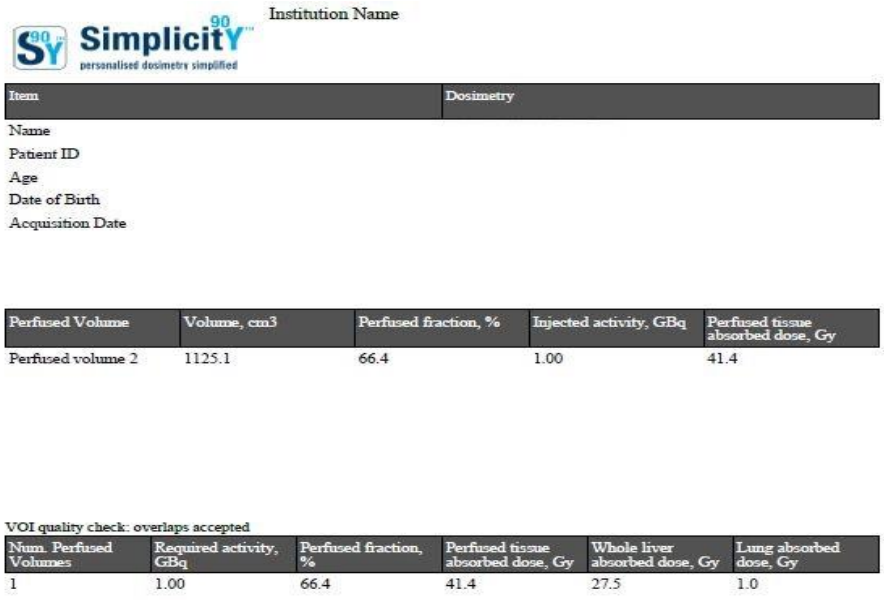

Institution Name

Item	Dosimetry
Name	
Patient ID	
Age	
Date of Birth	
Acquisition Date	

Perfused Volume	Volume, cm3	Perfused fraction, %	Injected activity, GBq	Perfused tissue absorbed dose, Gy
Perfused volume 2	1125.1	66.4	1.00	41.4

VOI quality check: overlaps accepted

Num. Perfused Volumes	Required activity, GBq	Perfused fraction, %	Perfused tissue absorbed dose, Gy	Whole liver absorbed dose, Gy	Lung absorbed dose, Gy
1	1.00	66.4	41.4	27.5	1.0

Figure 19 In this figure there is the first page of the Simplicity report

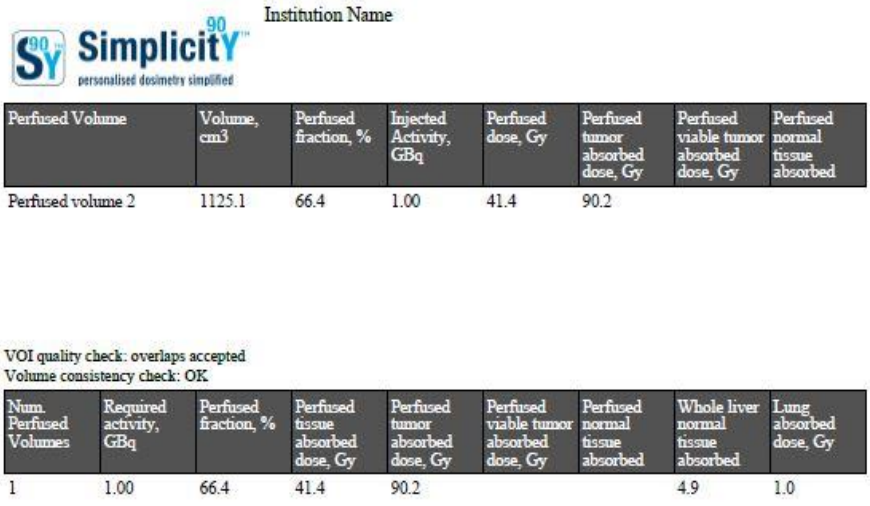

Institution Name

Perfused Volume	Volume, cm3	Perfused fraction, %	Injected Activity, GBq	Perfused dose, Gy	Perfused tumor absorbed dose, Gy	Perfused viable tumor absorbed dose, Gy	Perfused normal tissue absorbed
Perfused volume 2	1125.1	66.4	1.00	41.4	90.2		

VOI quality check: overlaps accepted
Volume consistency check: OK

Num. Perfused Volumes	Required activity, GBq	Perfused fraction, %	Perfused tissue absorbed dose, Gy	Perfused tumor absorbed dose, Gy	Perfused viable tumor absorbed dose, Gy	Perfused normal tissue absorbed	Whole liver normal tissue absorbed	Lung absorbed dose, Gy
1	1.00	66.4	41.4	90.2			4.9	1.0

Figure 20 This is the second page of the Simplicity report

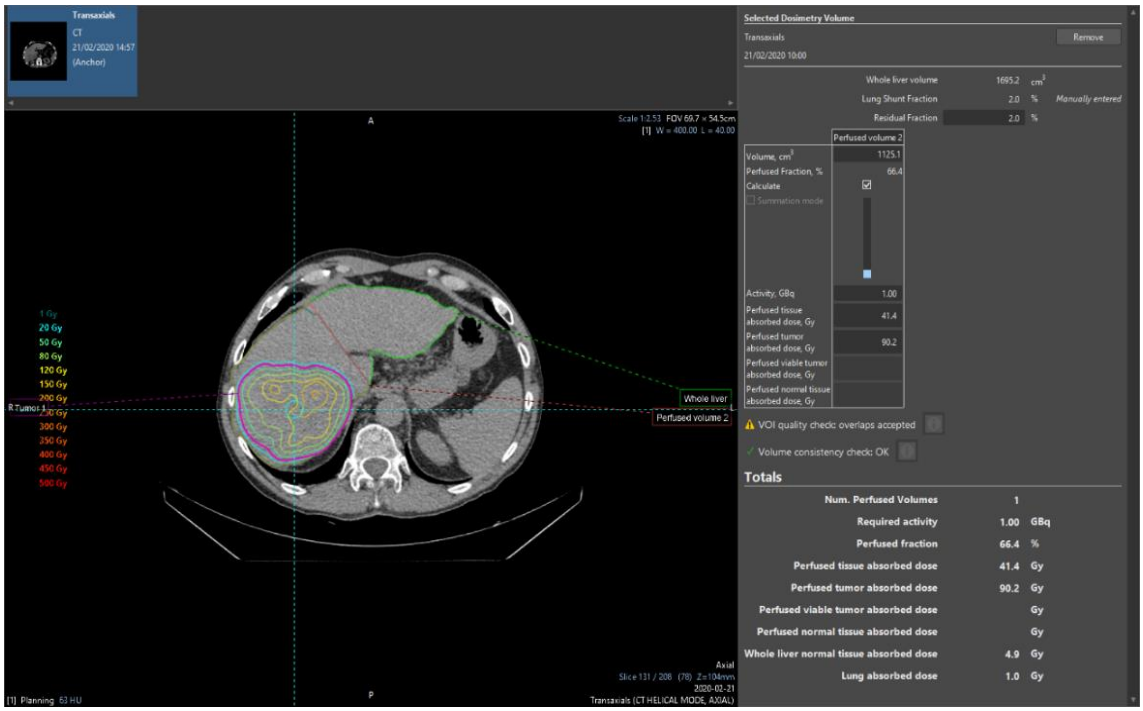

Figure 21 This is the second page of the Simplicity report

In the first page of the report there are listed the data of the patient in the initial frame, then there is the perfused volume, which is the treated volume, with the respectively administered activity. The other reported values are the administered activity in GBq and the absorbed doses of target lesion and whole liver in Gy. In the second page there are the absorbed doses for the perfused tissue and the tumour, for normal tissue and whole liver normal tissue. At the end of the report there is the tomographic image of the liver and the tumour area. Different colours indicate the different absorbed dose in the normal and tumour tissues.

These three listed methods are adopted to find the activity which should be dispensed to the tumour in a predictive phase.

Subsequently, a prospective analysis was carried out only for three patients of the predictive study. In the prospective scenario, after the ^{90}Y injection in the patient, Simplicit90Y was used to calculate the absorbed dose by normal and tumour tissue on post-treatment imaging with ^{90}Y PET/CT (Philips Vereos Digital PET/CT tomography), and it is shown in figure 22 [32].

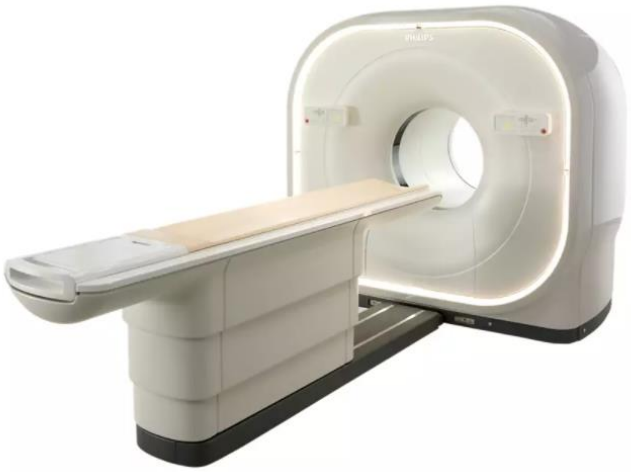

Figure 22 PET/CT [32]

In the figure 23 there is the report for the post-treatment evaluation, which includes the patient data, the ^{90}Y activity and the absorbed doses by normal and tumour tissues.

SimplicitY 90
personalised dosimetry simplified

Item	Dosimetry
Name	
Patient ID	
Age	
Date of Birth	
Acquisition Date	

Perfused Volume	Volume, cm3	Perfused fraction, %	Injected Activity, GBq	Perfused dose, Gy	Perfused tumor absorbed dose, Gy	Perfused viable tumor absorbed dose, Gy	Perfused normal tissue absorbed dose, Gy
Perfused volume 1	1064.1	62.6	1.60	72.1	157.8		68.4

VOI quality check: no overlaps detected
Volume consistency check: OK

Num. Perfused Volumes	Required activity, GBq	Perfused fraction, %	Perfused tissue absorbed dose, Gy	Perfused tumor absorbed dose, Gy	Perfused viable tumor absorbed dose, Gy	Perfused normal tissue absorbed dose, Gy	Whole liver normal tissue absorbed dose, Gy	Lung absorbed dose, Gy
1	1.60	62.6	72.1	157.8		68.4	42.2	1.0

Figure 23 Simplicity report for PET/CT

The statistical analysis was conducted to identify the differences between the three dosimetric methods in the retrospective analysis : the Kruskal-Wallis test, which is also called “one-way ANOVA on ranks”, was performed to carried out the comparison between several groups and to find if there are statistically significant differences [33]. This test can be applied when it is not possible to assume a normal distribution of the different groups. It is important to have at least three groups in this test because it is possible to detect the differences between two groups. This does not tell the precise differences among variables but gives a value called p-value.

The p-value is a probability which measures the evidence against null hypothesis. Lower probabilities provide strong evidence against null hypothesis [34]. This value is used to find if one of the differences between the medians are statistically significant [34]. If the p-value is small, lower than 0.05, the medians are not equal, and the differences are statistically significant.

Chapter 4

4 Results

4.1 Retrospective analysis

The different doses evaluated with the three dosimetric methods in the predictive analysis are reported in the following tables.

In the table 6 there are the administered activities of ^{90}Y -microspheres (GBq) and the respectively doses (Gy) calculated by MIRD method in normal lobe, lesion and normal liver, respectively.

Patients	Activity [GBq]	Dose MIRD [Gy]		
		Dose normal lobe	Dose lesion	Dose normal liver
#1	1,5	86,0	315,2	21,8
#2	3,3	15,2	186,0	12,4
#3	1,0	157,6	530,7	10,0
#4	2,0	29,4	243,9	30,2
#5	1,4	27,9	410,8	9,8
#6	2,5	54,8	220,4	10,7
#7	2,7	24,5	262,7	14,7
#8	2,5	36,7	106,8	6,8
#9	3,1	10,0	238,0	8,2
#10	1,9	17,3	295,3	17,5
#11	1,6	46,3	241,8	33,1
#12	3,5	22,2	226,5	18,0
#13	2,7	65,2	215,6	13,6

Table 6

In the table 7 are listed the administered activities of^{90}Y -microspheres (GBq) and the respectively doses (Gy) calculated by VOXEL method in normal lobe, lesion and normal liver, respectively.

Patients	Activity [GBq]	Dose VOXEL [Gy]		
		Dose normal lobe	Dose lesion	Dose normal liver
#1	1,5	93,0	337,7	23,5
#2	3,3	19,0	186,0	15,2
#3	1,0	166,1	553,4	10,6
#4	2,0	35,0	235,1	29,4
#5	1,4	29,1	405,1	10,2
#6	2,5	62,1	252,8	12,2
#7	2,7	25,8	267,7	15,4
#8	2,5	43,5	131,4	8,0
#9	3,1	10,2	233,5	8,3
#10	1,9	17,5	286,5	17,3
#11	1,6	45,2	228,9	32,4
#12	3,5	23,1	231,8	18,0
#13	2,7	75,7	249,5	15,8

Table 7

The table 8 contains the same data of the previous tables but the adopted method for the dosimetric evaluation was the Simplicity software.

Patients	Activity [GBq]	Dose Simplicity [Gy]		
		Dose normal lobe	Dose lesion	Dose normal liver
#1	1,5	40,6	226,1	18,5
#2	3,3	29,8	71,3	7,8
#3	1,0	46,4	415,0	16,9
#4	2,0	41,5	76,7	31,9
#5	1,4	102,0	496,0	6,7
#6	2,5	41,4	90,2	4,9
#7	2,7	39,2	136,0	15,9
#8	2,5	30,7	461,5	12,7
#9	3,1	73,3	243,3	7,6
#10	1,9	33,2	150,9	11,9
#11	1,6	72,1	317,1	38,1
#12	3,5	79,5	257,1	20,2
#13	2,7	138,6	341,9	21,2

Table 8

The absorbed dose limits are observed, and it is possible to see from the tables the absorbed dose from the tumour tissue. Since the absorbed dose for the tumour should be higher than 200 Gy to be effective, here it is noticed that about all values are above 200 Gy. In some cases, despite the high activities, the absorbed dose from the lesion is smaller than the value obtained with lower activity. This phenomenon depends on the tumour mass. For the same administered activity, if the tumour mass is broader the absorbed dose is smaller than the one related to a larger tumour mass. Remembering the equation 27 for the evaluation of the absorbed dose in the tumour, there is an inversely proportion between the dose and the mass of the tumour. It means that the bigger the mass the smaller the dose and conversely. Moreover, for the healthy liver the absorbed dose depends on the mass of the tissues.

To perform the Kruskal-Wallis test it is used a Monte Carlo method on MATLAB, which is useful to interpret and report the obtained results [33].

In the table 9 there is a summary of the data for the three methods including minimum, median and maximum value of the absorbed dose in normal lobe, in target lesion and in normal liver, respectively. There is also the percentile dose (25 and 75) for the three methods.

		lobe method			site lesion method			liver method		
		MIRD	VOXEL	SIMPL	MIRD	VOXEL	SIMPL	MIRD	VOXEL	SIMPL
dose	Minimum	10	10	30	107	131	71	7	8	5
	Percentile 25	22	23	39	220	232	136	10	11	8
	Median	29	35	42	242	250	243	14	15	16
	Percentile 75	55	62	73	295	287	342	18	18	20
	Maximum	158	166	139	531	553	496	33	32	38

Table 9

With a boxplot there are reported graphically these data to show the different dose intervals in the three methods and to make a comparison. There is one graph for the different compartments: the normal lobe, the lesion, and the normal liver. The graph in the figure 24 is for the normal lobe. The three methods are in the abscissa axes, in the ordinate there are the absorbed dose values.

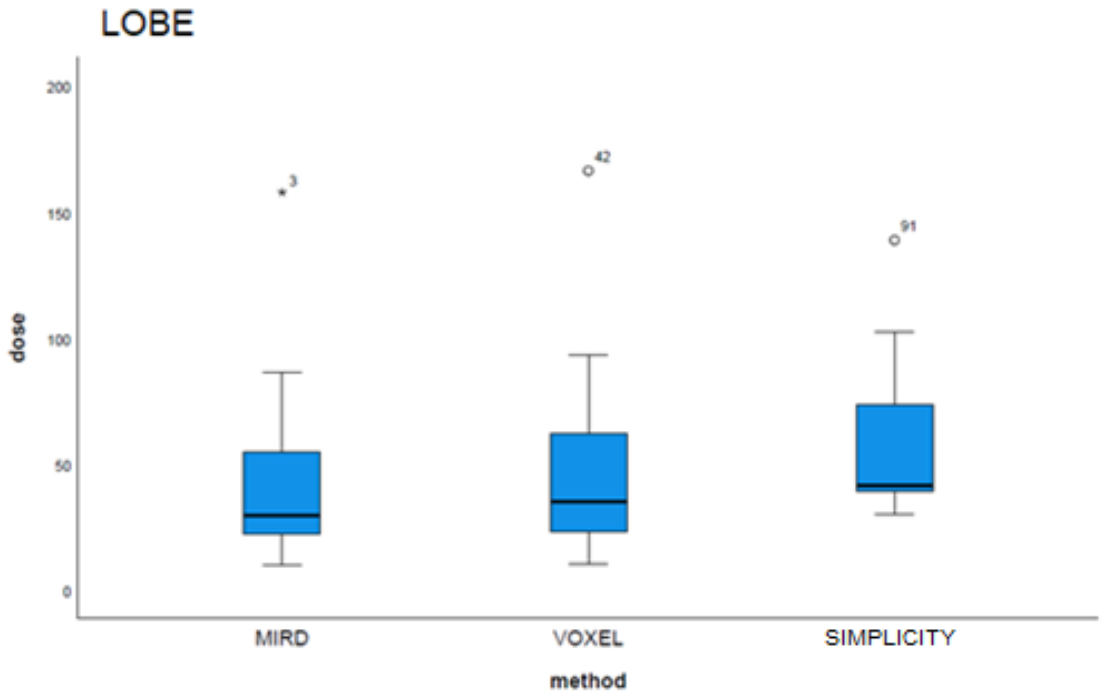

Figure 24 Boxplot for the normal lobe

It is possible to notice that the three methods have about the same median value of the delivered dose. The range of the third method is different from the other two. The lower and the upper edges of the blue box represent respectively the 25 and the 75 percentiles. The minimum dose in Simplicity, which is represented by the lower black bar, is higher than the value in MIRD and VOXEL. The maximum value of the dose in Simplicity, which is represented by the upper black bar, is lower than the dose evaluated with MIRD and VOXEL methods. Moreover, the 25 percentile is higher in the Simplicity method compared to the other two, and also the 75 percentile. Between the 25 and 75 percentile there are the normal values, which include the 50% of the observation.

The Kruskal-Wallis test did not find any significant differences between MIRD, VOXEL and Simplicity methods (p=0.19). The results are shown in table 10. Since the p-value is higher than 0.05 (5%) there are no significant differences between the three methods.

Test Statistics[a,b]

			dose
Kruskal-Wallis H			3,338
df			2
Asymp. Sig.			,188
Monte Carlo Sig.	Sig.		,196[c]
	99% Confidence Interval	Lower Bound	,186
		Upper Bound	,207

a. Kruskal Wallis Test

b. Grouping Variable: method

c. Based on 10000 sampled tables with starting seed 112562564.

Table10

Moving to the next analysed compartment, in figure 25 is illustrated the boxplot for the lesion absorbed dose. The absorbed doses from the lesion are higher than the absorbed doses from the healthy lobe. This discrepancy is evident because the aim of the treatment is to irradiate the tumour volume more than the normal liver, indeed minimize the absorbed dose from other tissues.

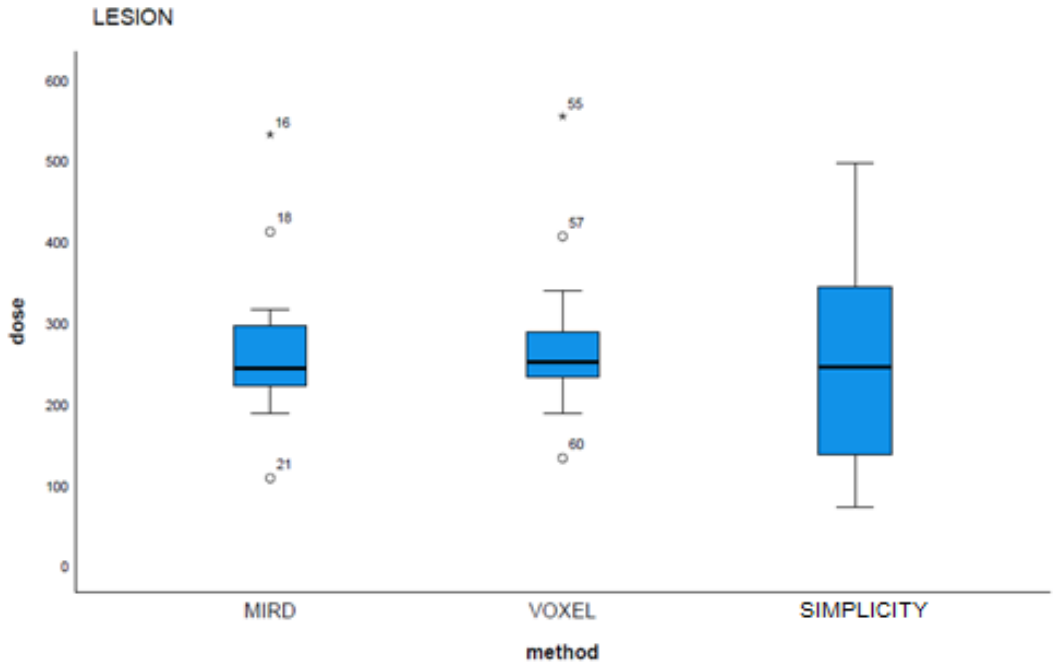

Figure 25 Boxplot for the lesion

Also for the lesion absorbed dose, the Kruskal-Wallis test did not find any significant differences between MIRD, VOXEL and Simplicity methods (p=0.86). The results are shown in table 11.

Test Statistics[a,b]

			dose
Kruskal-Wallis H			,296
df			2
Asymp. Sig.			,863
Monte Carlo Sig.	Sig.		,862[c]
	99% Confidence Interval	Lower Bound	,853
		Upper Bound	,871

a. Kruskal Wallis Test

b. Grouping Variable: method

c. Based on 10000 sampled tables with starting seed 221623949.

Table 11

The last examined compartment with the three methods is the normal liver. The relative boxplot is shown in figure 26.

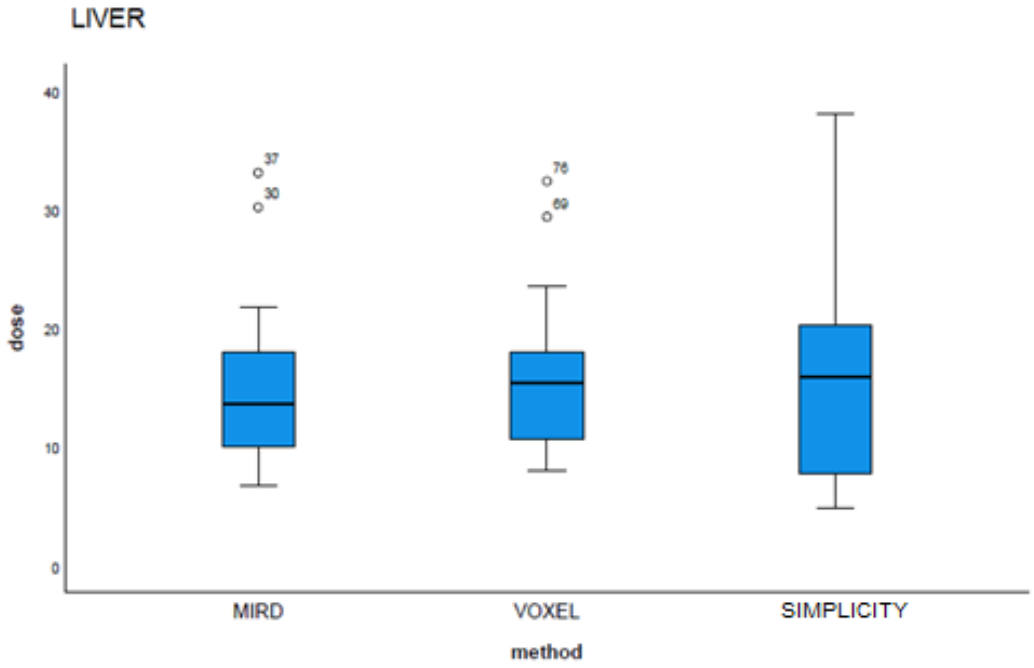

Figure 26 Boxplot for the normal liver

The Kruskall-Wallis test results are in the table 12. The p-value is 0.94 and it means that the differences between the three methods are not statistically significant since p is higher than 0.05.

Test Statistics[a,b]

			dose
Kruskal-Wallis H			,118
df			2
Asymp. Sig.			,943
Monte Carlo Sig.	Sig.		,943[c]
	99% Confidence Interval	Lower Bound	,937
		Upper Bound	,949

a. Kruskal Wallis Test

b. Grouping Variable: method

c. Based on 10000 sampled tables with starting seed 303130861.

Table 12

4.2 Prospective analysis

The prospective analysis was performed in only three patients that underwent a post-treatment ^{90}Y PET/CT scan and subsequent post-treatment dosimetric evaluation: all PET/CT scans were acquired with the Philips Vereos Digital PET/TC tomograph exploiting the very low decay ratio β+ of 90Y (32:1000000). After CT scout, PET/TC images were acquired from 2 bed per patient, each lasting 12 minutes, with the liver in the centre of the 2 bed positions. In the figure 27, in the chart are reported the normal lobe, lesion and normal liver absorbed dose calculated by Simplicity® in the pre and post-treatment dosimetric evaluation with ^{99m}Tc-MAA SPECT/CT and ^{90}Y PET/CT scan, respectively.

There is apparent slight difference between pre and post-treatment absorbed dose in the lesion compartment, especially for the patient number 11. Since in post-treatment dosimetry it is employed PET/CT, should be considered that the yttrium-90 needs more time to emit a significant number of photons. The standard acquisition time for the PET exam is about 12 minutes. If the administered activity is small as in the examined case, it is mandatory to expand the acquisition time to have a better signal capture.

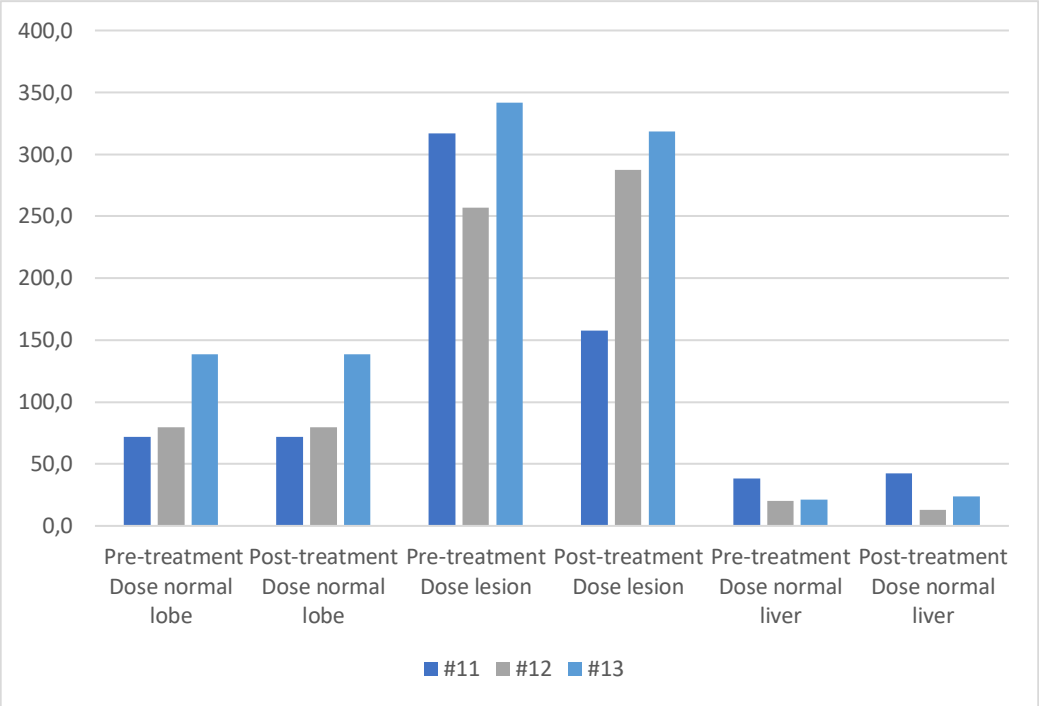

Figure 27 This chart shows the comparison between pre-treatment and post-treatment absorbed dose in the normal lobe, in the lesion, and in normal liver.

The differences present among pre-treatment and post-treatment are generated by the different employed isotopes. Technetium-99m and yttrium-90 have different decays and the acquisition time in the imaging should depend on the injected activity. Another point that can make differences between pre-treatment and post-treatment dosimetric evaluation is the position of the catheter. It is assumed that for the two different isotopes the catheter has the same position, however there are not perfectly aligned. Moreover, the planned activity with technetium-99m is the same of the administered activity with yttrium-90.

Discussion

This study was focused on the reproducibility of dosimetric evaluation in nuclear medicine therapy. In particular, the trans-arterial radioembolization with ^{90}Y-microspheres has been used as a model for the comparison among different evaluation methods.

In trans-arterial radioembolization the different dosimetric methods are proposed by the microsphere manufacturers. Several methods are adopted for pretherapeutic ^{99m}Tc-MAA scintigraphy based dosimetry; for resin spheres based on the body surface area, for glass spheres based on mono-compartmental, which does not consider the different compartment of the liver (tumour and normal tissue) [17].

In this work only patients with HCC treated with glass microspheres have been included for a total of 13 patients for pre-therapeutic dosimetry and 3 with also post-therapeutic ^{90}Y PET based dosimetry. The analysis was driven by three different methods: multi-compartmental MIRD and convolution based VOXEL dosimetry on Matlab, and the commercial available Simplicity software (distributed by MIRDA Accelerating Cancer Care).

The importance of dosimetry in therapeutical nuclear medicine it is related to the need to establish the relationship between absorbed doses in treated lesions and medical effects to forecast the results in term of response to therapy. Several studies highlight this correlation and the relevance of carrying out a personalized dosimetric approach for each patient [17]. Chiesa et al. [35] found that the dose distribution at voxel level exceed the normal procedure. Another point of view is suggested by Garin et al. [36] which have calculated the doses of normal liver and tumour with a quantitative analysis of ^{99m}Tc-MAA applied on 36 patients affected by HCC. The outcome of this study was the strong correlation between patient response and the absorbed dose [17]. It was demonstrated by Garin at al. [37] that ^{99m}Tc-MAA SPECT/CT dosimetry imaging was able to forecast the presence of response and duration on 71 patients treated with glass spheres [17].

Performing dosimetry comparison between pre-treatment and post-treatment, it is still an issue to understand if the doses planned and the doses administered are concordant. A study was conducted by Richetta et al. [38] for a comparison between ^{99m}Tc-MAA SPECT/CT and ^{90}Y PET/CT on a group of 10 patients, which stressed the congruence

between the activity planned and the activity administered. But the reproducibility and predictability of post-treatment absorbed dose pretherapeutic ^{99m}Tc-MAA dosimetric based analysis is still under evaluation. The study made by Gnesin [39] on 27 patients has underlined that the absorbed dose predicted by ^{99m}Tc-MAA SPECT/CT is confirmed by the absorbed dose evaluate in post-treatment ^{90}Y PET/CT [38]. Differing opinion is still present in a study made by Haste [40] where it is found a correlation between the catheter mismatch in pre-treatment and post-treatment, and the absorbed dose imbalance between pre-therapeutic SPECT/CT and post-therapeutic PET/CT imaging [38]. Nevertheless, there is the need to identify the best methodology to perform dosimetry before radioembolization.

In our study predictive dosimetric examination was performed with three methods (MIRD, VOXEL and Simplicity) and there were not relevant discrepancies between them ($p=0.19$ normal lobe, $p=0.86$ lesion, $p=0.94$ normal liver).

Based on the prospective analysis of 3 patients small differences comes out between the pre-treatment and post-treatment dosimetry. This is maybe due to the different injected isotopes and the different catheter positioning. However, only one patient has significant discrepancy between the absorbed lesion dose evaluated by ^{99m}Tc-MAA SPECT/CT and ^{90}Y PET/CT, so the predictive evaluation with ^{99m}Tc-MAA is reliable.

Furthermore, in our sample study the safety and the effectiveness of the ^{90}Y-TARE were analysed, and the dosimetric limits have been respected. Therefore, the delivered dose for the tumour was higher than 200 Gy, for the normal liver lower than 120 Gy and the lung shunt fraction was smaller than 30 Gy. However, therapy was effective for treated patients.

The directive 2013/59 EURATOM explains the importance of the dosimetric evaluation in nuclear medicine and the results of this thesis work strengthen this concept. Although the dosimetric analysis is complex and there are needed specialized operators to perform all procedures. In some cases it is not feasible, the availability of the patient and time are requested.

Conclusions

The obtained results from the analysis underline the importance of the dosimetric evaluations in the radioembolization treatment in patients with hepatocellular carcinoma (HCC), focusing on ^{90}Y-microspheres approach. The dosimetric analysis helps to prepare the patient to the treatment but also to predict response after therapy.

In this work the three analysed dosimetric methods (MIRD, VOXEL and Simplicity®) are all accurate for the dosimetry evaluation. The choice of one method rather than another depends on the availability of the software in the hospital. MIRD is available in all hospitals. The VOXEL method is not achieved in all hospitals. However, it is commonly used MIRD because VOXEL is more complex to perform. The last applied method is Simplicity, which is a software developed by manufacturers of Theraspheres, not opensource and not available in all centres. Finally, according to very preliminary results the ^{99m}Tc-MAA scintigraphy base dosimetry seems to well predict the post-therapeutic absorbed dose if the treatment is performed in the same conditions to pre-therapeutic procedures.

Our study, even if including a small sample size, supported by international scientific literature, indicate that dosimetry in TARE is feasible through different methods, the method to be used is not related to the efficacy of the treatment but more to the availability of dedicated operators with implementation of safety and radiation protection in Nuclear Medicine.

Bibliography

[1] Guenther Dietze et al., «International Commission on radiological protection committee 2 basis for dosimetric quantities used in radiological protection».

[2] D. Akata et al., «Summary of the European Directive 2013/59/Euratom: essentials», 2015.

[3] «EASL Clinical Practice Guidelines: Management of hepatocellular carcinoma», *Jurnal of hepatology ,* p. 182–236, 2018.

[4] Carlo Chiesa et al., «Documento di consensus intersocietario a cura dell'associazione italiana di fisica medica e associazione italiana di medicina nucleare terapia medico nucleare: ottimizzazione su base dosimetrica ai sensi della direttiva europea 2013/59/EURATOM».

[5] «https://www.cancer.gov/about-cancer/treatment/types/radiation-therapy#:~:text=At%20high%20doses%2C%20radiation%20therapy,and%20removed%20by%20the%20body» [Online].

[6] «https://www.cancer.org/treatment/treatments-and-side-effects/treatment-types/radiation/systemic-radiation-therapy.html» [Online].

[7] Stephen Joseph McMahon, «The linear quadratic model: usage, interpretation and challenges».

[8] S. Peter Kima et al., «A guide to 90Y radioembolization and its dosimetry», 2019.

[9] David A. Weber, «The Mird method of estimating absorbed dose».

[10] Ben J. Tickner et al., «The use of yttrium in medical imaging and therapy: historical background and future perspectives», 2020.

[11] Dash et al., « Radiopharmaceuticals for therapy», Springer, 2016.

[12] Tong A et al., «Yttrium-90 hepatic redioembolization: clinical review and current techniques in interventional radiology and personalized dosimetry», 2016.

[13] M. D'Arienzo, «Emission of β+ particles via internal pair production in the 0+ – 0+ transition of 90Zr: historical background and current applications in nuclear medicine imaging», 2013.

[14] «https://www.ema.europa.eu/en/documents/scientific-discussion/yttriga-epar-scientific-discussion_en.pdf» [Online].

[15] IAEA, «Yttrium-90 And Rhenium-188 radiopharmaceuticals for radionuclide therapy», 2015.

[16] Francesco Giammarile et al.,«EANM procedure guideline for the treatment of liver cancer and liver metastases with intra-arterial radioactive compounds», 2011.

[17] Elena Gallio et al., «Calculation of tumour and normal tissue biological effective dose in 90Y liver radioembolization with different dosimetric methods», 2016.

[18] «https://www.cancer.org/cancer/liver-cancer/treating/embolization-therapy.html».

[19] «https://www.ehealthstar.com/anatomy/liver» [Online].

[20] Amirtahà Taebi et al., «Computational modeling of the liver arterial blood flow for microsphere therapy: effect of boundary conditions», 2020.

[21] «https://www.radiologyinfo.org/en/info/angiocath» [Online].

[22] «https://en.wikipedia.org/wiki/Angiography#/media/File:Herzkatheterlabor_modern.jpeg» [Online].

[23] «https://youtu.be/YJ4SiUYSzNY» [Online].

[24] «https://medicine.umich.edu/dept/radiology/research/pet-center» [Online].

[25] «https://www.nibib.nih.gov/science-education/science-topics/nuclear-medicine#:~:text=The%20main%20difference%20between%20SPECT,an%20electron%20but%20oppositely%20charged» [Online].

[26] «https://www.dicardiology.com/product/ge-introduces-discovery-nmct-670-pro-and-qmetrix» [Online].

[27] Riad Salem et al., «Clinical and dosimetric considerations for Y90: recommendations», 2019.

[28] Gulec Seza et al., «Dosimetric techniques in 90Y-microsphere therapy of liver cancer: the MIRD equation for dose calculations», *Jurnal of Nuclear Medicine,* 2006.

[29] Lanconelli N et al., «A free database of radionuclide voxel S values for the dosimetry of nonuniform activity distribution», 2012.

[30] «https://mirada-medical.com/product/simplicit90y-dosimetry-planning/» [Online].

[31] Simplicit^{90}Y 2.4 Help Guide.

[32] «https://www.usa.philips.com/healthcare/product/HC882446/vereos-digital-petct-proven-accuracy-inspires-confidence» [Online].

[33] «https://statistics.laerd.com/spss-tutorials/kruskal-wallis-h-test-using-spss-statistics.php» [Online].

[34] «https://support.minitab.com/en-us/minitab/19/help-and-how-to/statistics/nonparametrics/how-to/kruskal-wallis-test/interpret-the-results/all-statistics/» [Online].

[35] Chiesa C et al., «Need, feasibility and convenience of dosimetric treatment planning in liver selective internal radiation therapy with 90Y microspheres: the experience of the National Tunor Institute of Milano», *Q J Nucl Med Mol Imaging,* 2011.

[36] Garin E. et al., «Dosimetry based on 99mTc-MAA SPECT/CT based dosimetry accurately predicts tumour response and survival in HCC patients treated with 90T-loaded glass microspheres: preliminary results», *J Nucl Med,* 2012.

[37] Garin E. et al., «Boosted selective internal radiation therapy with 90Y-loaded glass microspheres (B-SIRT) for hepatocellular carcinoma patients: a new personalized promising concept», *European Journal of Nuclear Medicine and Molecular Imaging volume ,* 2013.

[38] Elisa Richetta et al., «PET-CT post therapy dosimetry in radioembolization with resin 90Y microspheres: Comparison with pre-treatment SPECT-CT 99mTc-MAA results», *Physica Medica,* 2019.

[39] Gnesin S. et al., «Partition model-based 99mTc-MAA SPECT/CT predictive dosimetry compared with 90Y TOF PET/CT post treatment dosimetry in

radioembolization of hepatocellular carcinoma: a quantitative agreement comparison», J Nucl Med, 2016.

[40] Haste P. et al., «Correlation of technetium-99m macroaggregated albumin and yttrium-90 glass microsphere biodistribution in hepatocellular carcinoma:a retrospective review of pretreatment single photon emission CT and posttreatment positron emission tomography/CT», J Vasc Interv Radiol, 2017.